

**EFFECT OF ELECTRIC FIELD DISTRIBUTION OF POLYMER  
NANOCOMPOSITES UNDER DIFFERENT FILLER SIZE USING  
FEMM 4.2 SOFTWARE**



**BALQIS BINTI ROSLI**

**BACHELOR OF ELECTRICAL ENGINEERING WITH HONOURS  
UNIVERSITI TEKNIKAL MALAYSIA MELAKA**

**2024**

**EFFECT OF ELECTRIC FIELD DISTRIBUTION OF POLYMER  
NANOCOMPOSITES UNDER DIFFERENT FILLER SIZE USING FEMM 4.2  
SOFTWARE**

**BALQIS BINTI ROSLI**



**UNIVERSITI TEKNIKAL MALAYSIA MELAKA**

**2024**

## DECLARATION

I declare that this thesis entitled "EFFECT OF ELECTRIC FIELD DISTRIBUTION OF POLYMER NANOCOMPOSITES UNDER DIFFERENT FILLER SIZE USING FEMM 4.2 SOFTWARE is the result of my own research except as cited in the references. The thesis has not been accepted for any degree and is not concurrently submitted in the candidature of any other degree.

Signature :



Name :

BALQIS BINTI ROSLI

Date :

21/06/2024

UNIVERSITI TEKNIKAL MALAYSIA MELAKA

## APPROVAL

I hereby declare that I have checked this report entitled "title of the project", and in my opinion, this thesis fulfils the partial requirement to be awarded the degree of Bachelor of Electrical Engineering with Honours

Signature :

Supervisor Name :

TS. DR. NOR HADAYAH BINTI RAHIM

Date :

21/06/2024

اونيورسيتي تيكنيكل مليسيا ملاك  
UNIVERSITI TEKNIKAL MALAYSIA MELAKA

## DEDICATIONS

First and foremost, thank you Allah, the Most Gracious and Most Merciful, whose guidance has been my constant source of strength throughout this academic journey. In gratitude, I extend my deepest appreciation to my beloved parents for their unwavering support, sacrifices, and encouragement. To my supervisor, Ts. Dr. Nor Hidayah Binti Rahim, your wisdom and guidance have been instrumental in shaping this project and my academic growth. I am immensely thankful to my friends for their support, making both challenges and triumphs more meaningful. To my family, your love and understanding have been my anchor. This project is also dedicated to the academic community at Universiti Teknikal Malaysia Melaka (UTeM) and all those who have contributed to my learning. To Allah, I express my gratitude for the blessings that have made this achievement possible.

## ACKNOWLEDGEMENTS

I am forever grateful to Allah the almighty for all the blessings He has given me throughout my life. Indeed, He is the best planner and I'm thankful for all his arrangements that he has and will plan for me. I would like to extend my heartfelt gratitude to all those who have contributed to the successful completion of my Final Year Report 1. First and foremost, I am deeply thankful to the following individuals and organizations:

Dr. Nor Hidayah Binti Rahim as my supervisor for her guidance, unwavering support, and invaluable insights throughout the project. Her expertise and encouragement have been instrumental in shaping the direction of this research.

My panelists, Dr. Nur Zawani Binti Saharuddin and Dr. Nur Hakimah Binti Ab. Aziz for their guidance, insightful feedback and constructive comments. Their expertise and insights have been instrumental in shaping this report. Additionally, I acknowledge the Faculty of Electrical Engineering (UTeM) for granting me the opportunity to pursue this project and for providing excellent facilities, including a well-equipped lab that greatly facilitated my work.

My academic coordinator: Ts. Dr. Ezreen Farina Binti Shair for their continuous guidance and coordination. Their guidance has been crucial in ensuring the smooth progress of this project and navigating the academic requirements.

Family and Friends: My family and friends deserve special mention for their constant encouragement, patience, and understanding during this challenging period. Your belief in me has been a driving force.

This report is a culmination of the collective efforts and support from all of you. Thank you for being an integral part of this academic endeavor.

## ABSTRACT

High voltage insulation holds significant importance in the realm of electrical systems, playing a crucial role in ensuring the safety, reliability, and efficiency of power transmission and distribution networks. Polymer nanocomposites, when used as insulating materials, have shown promising properties for applications in electrical insulation. These ingenious materials, formed by incorporating nanofillers (typically ranging from 1 to 100 nanometers in size) into a polymer matrix, offer a captivating blend of enhanced properties, with the distribution of the electric field playing a crucial role in their performance. However, the distribution of electric fields within these composite materials is also affected by filler characteristics such as size and concentration. In this study, finite element modelling was used to investigate the effect of nanoparticle size on electric field distribution in polymer nanocomposites. Polyethylene matrix composites containing spherical silica nanoparticles of sizes ranging from 20nm, 40nm, 60nm, 80nm and 100nm were modelled and simulated using FEMM 4.2 finite element software. An interphase region between the nanoparticle and matrix was also included. For this project, the interphase used were 10nm and 20nm. Simulation results showed that electric field intensity increased with larger nanoparticle sizes. The electric field distribution is a critical aspect of high voltage insulator performance, as it directly influences the material's ability to withstand electrical stress. Hence, it can be concluded that by increasing the nanoparticle size will increase electric field intensity. The increment of electric field intensity could affect the or lead the tendency of material to breakdown.

## ***ABSTRAK***

Penebat voltan tinggi mempunyai kepentingan yang signifikan dalam sistem elektrik, memainkan peranan penting dalam memastikan keselamatan, kebolehpercayaan, dan kecekapan rangkaian penghantaran dan pengagihan kuasa. Nanokomposit polimer, apabila digunakan sebagai bahan penebat, menunjukkan sifat-sifat yang menjanjikan untuk aplikasi dalam penebat elektrik. Bahan-bahan yang inovatif ini, yang dibentuk dengan menggabungkan pengisi nano (biasanya dalam lingkungan 1 hingga 100 nanometer saiznya) ke dalam matriks polimer, menawarkan gabungan sifat-sifat yang dipertingkatkan, dengan pengagihan medan elektrik memainkan peranan penting dalam prestasinya. Walau bagaimanapun, pengagihan medan elektrik dalam bahan komposit ini juga dipengaruhi oleh ciri-ciri pengisi seperti saiz dan kepekatan. Dalam kajian ini, pemodelan unsur terhingga digunakan untuk menyiasat kesan saiz nanopartikel ke atas pengagihan medan elektrik dalam nanokomposit polimer. Komposit matriks polietilena yang mengandungi nanopartikel silika sfera dengan saiz antara 20nm, 40nm, 60nm, 80nm dan 100nm telah dimodelkan dan disimulasikan menggunakan perisian unsur terhingga FEMM 4.2. Satu kawasan antara fasa antara nanopartikel dan matriks juga disertakan. Untuk projek ini, kawasan antara fasa yang digunakan adalah 10nm dan 20nm. Hasil simulasi menunjukkan bahawa keamatan medan elektrik meningkat dengan saiz nanopartikel yang lebih besar. Pengagihan medan elektrik adalah aspek kritikal dalam prestasi penebat voltan tinggi, kerana ia secara langsung mempengaruhi keupayaan bahan untuk menahan tekanan elektrik. Oleh itu, dapat disimpulkan bahawa dengan meningkatkan saiz nanopartikel akan meningkatkan keamatan medan elektrik. Peningkatan keamatan medan elektrik boleh mempengaruhi atau menyebabkan kecenderungan bahan untuk mengalami kerosakan.



## TABLE OF CONTENTS

	<b>PAGE</b>
<b>DECLARATION</b>	
<b>APPROVAL</b>	
<b>DEDICATIONS</b>	
<b>ACKNOWLEDGEMENTS</b>	<b>2</b>
<b>ABSTRACT</b>	<b>3</b>
<b>ABSTRAK</b>	<b>4</b>
<b>TABLE OF CONTENTS</b>	<b>5</b>
<b>LIST OF TABLES</b>	<b>7</b>
<b>LIST OF FIGURES</b>	<b>8</b>
<b>LIST OF SYMBOLS AND ABBREVIATIONS</b>	<b>12</b>
<b>CHAPTER 1 INTRODUCTION</b>	<b>13</b>
1.1 Background	13
1.2 Motivation	14
1.3 Problem Statement	14
1.4 Objectives	15
1.5 Scope of Work	15
1.6 Thesis Outline	16
<b>CHAPTER 2 LITERATURE REVIEW</b>	<b>17</b>
2.1 Introduction	17
2.2 High Voltage Insulator	17
2.3 Polymer Nanocomposites	18
2.4 Polymer	21
2.5 Nanoparticle / Nanofiller	22
2.6 Interphase	24
2.7 Tanaka's Multi Core Model	26

2.8	Literature Review on The Simulation of Model Nanocomposites	28
<b>CHAPTER 3 METHODOLOGY</b>		<b>37</b>
3.1	Introduction	37
3.2	Project Flow	37
3.3	K-Chart	39
3.4	Finite Element Method Magnetics (FEMM) 4.2 Software	39
3.5	Polymer Nanocomposites Modelling	40
3.6	Finite Element Method Magnetics (FEMM) 4.2 Software Setting	42
<b>CHAPTER 4 RESULTS AND DISCUSSIONS</b>		<b>49</b>
4.1	Introduction	49
4.2	Unfilled Polyethylene (PE)	49
4.3	Polyethylene Nanocomposites at Different Filler Size at 10nm Interphase	50
4.3.1	PE at 20nm nanoparticle with 10nm interphase	50
4.3.2	PE at 40nm nanoparticle with 10nm interphase	52
4.3.3	PE at 60nm nanoparticle with 10nm interphase	53
4.3.4	PE at 80nm nanoparticle with 10nm interphase	55
4.3.5	PE at 100nm nanoparticle with 10nm interphase	56
4.4	Polyethylene Nanocomposites at Different Filler Size at 20nm Interphase	58
4.4.1	PE at 20nm nanoparticle with 20nm interphase	58
4.4.2	PE at 40nm nanoparticle with 20nm interphase	59
4.4.3	PE at 60nm nanoparticle with 20nm interphase	61
4.4.4	PE at 80nm nanoparticle with 20nm interphase	62
4.4.5	PE at 100nm nanoparticle with 20nm interphase	64
<b>CHAPTER 5</b>		<b>68</b>
5.1	Conclusion	68
5.2	Future Work	68
<b>REFERENCES</b>		<b>70</b>

## LIST OF TABLES

Table 2.1: Models and parameter [39]	34
Table 3.1: Modelling parameters of the materials	41
Table 4.1: Summary of the results	66



## LIST OF FIGURES

Figure 2.1: Common geometries and reinforcing of particles in nano- and macro-composites [2]	19
Figure 2.2: Formation of thermoplastic, elastomer and thermoset [27]	21
Figure 2.3: Formation of thermoplastic elastomer [28]	22
Figure 2.4: Common particle reinforcements/geometries and their respective surface area-to-volume ratios R [2]	24
Figure 2.5: Interphase concept in polymer nanocomposites [33]	25
Figure 2.6: Tanaka's Multi Core Model [37]	26
Figure 2.7: A 2D unit cell model ( $1\ \mu\text{m} \times 1\ \mu\text{m}$ ) of a nanocomposite consisting of a polymer, a nanoparticle, and an interphase, positioned between a high voltage electrode and a ground electrode [37]	28
Figure 2.8: Effect of (a) nanoparticle (without interphase) on the electric field intensity plots along the (b) $90^\circ$ vertical line and (c) $0^\circ$ horizontal line, originating from the center of the nanoparticle and extending into the polymer region [37]	29
Figure 2.9: Five different random distributions of ceramic particles in polymer matrix from (a) to (e); (f) to (j) is the distribution of electric field strength corresponding to each random distribution [38]	30
Figure 2.10: Weibull plots comparing the DC breakdown strength of (a) LDPE, (b) HDPE containing 0 wt%, 1 wt%, 3 wt%, and 5 wt% of nanosilica [39]	32

Figure 2.11: Weibull plots comparing the AC breakdown strength of (a) LDPE, (b) HDPE containing 0 wt%, 1 wt%, 3 wt%, and 5 wt% of nanosilica [39]	33
Figure 2.12: A 2D unit cell model (1 mm × 1 mm) of a nanocomposite consisting of a polymer, a nanoparticle, and an interphase, situated between a high voltage electrode and a ground electrode[39]	34
Figure 2.13(a): Illustration of a nanocomposite with an interphase. The vertical (y-line) and horizontal (x-line) lines indicate the locations where electric field intensity data were collected for Nano Model I. (b) Depiction of a nanocomposite with nanoparticles and interphases, with the nanoparticles separated by a defined interparticle distance [39]	35
Figure 3.1: Flowchart of the project	38
Figure 3.2: K-Chart of the project	39
Figure 3.3: A two-dimensional polymer slab with dimension of 1 μm x 1 μm	40
Figure 3.4: Finite Element Method Magnetic (FEMM) 4.2 display	42
Figure 3.5: Create New Problem Dialog	42
Figure 3.6: Problem Definition dialog	43
Figure 3.7: tool bar buttons	43
Figure 3.8: Materials Library dialog	44
Figure 3.9: Block Property dialog for materials	44
Figure 3.10: Block Property dialog for boundary	45
Figure 3.11: Block Property for coordinate point	45
Figure 3.12: Mesh size parameter dialog	46
Figure 3.13: Nanocomposites Modelling	46

Figure 3.14: Toolbar buttons for starting analysis tasks	47
Figure 3.15: Display result in voltage (V)	47
Figure 3.16: Buttons that facilitate the analysis of the simulated model	48
Figure 3.17: Field intensity display (V/m)	48
Figure 4.1: Intensity Color Contour of Unfilled PE	49
Figure 4.2: Graph	50
Figure 4.3 (a)	51
Figure 4.3 (b)	52
Figure 4.4 (a)	53
Figure 4.4 (b)	53
Figure 4.5 (a)	54
Figure 4.5 (b)	54
Figure 4.6 (a)	55
Figure 4.6 (b)	56
Figure 4.7 (a)	57
Figure 4.7 (b)	57
Figure 4.8 (a)	59
Figure 4.8 (b)	59
Figure 4.9 (a)	60
Figure 4.9 (b)	60
Figure 4.10 (a)	61
Figure 4.10 (b)	62
Figure 4.11 (a)	63
Figure 4.11 (b)	63
Figure 4.12 (a)	64

Figure 4.12(b)

65

Figure 4.13: Comparison of different nanoparticle sizes at interphase of 10nm

and 20nm

67



## LIST OF SYMBOLS AND ABBREVIATIONS

Electric field	-	E-field
SiO <sub>2</sub>	-	Silicon Dioxide/Silica
ZnO	-	Zinc Oxide
Al <sub>2</sub> O <sub>3</sub>	-	Aluminium Oxide
TiO <sub>2</sub>	-	Titanium Oxide
CNTs	-	Carbon Nanotubes
TEM	-	Transmission electron microscopy
FEMM	-	Finite Element Method Magnetics
2D	-	2 Dimension
HDPE	-	High-density polyethylene
LDPE	-	Low-density polyethylene
AC	-	Alternating current
DC	-	Direct current
T <sub>g</sub>	-	Transmission temperature
D,d	-	Diameter
wt%	-	Weight percentage
nm	-	nanometer
μm	-	micrometer
L	-	Length
h	-	Height
R	-	Surface area-to-volume ratios
ξ	-	Xi
E	-	Electric Field Intensity
V	-	Voltage
kV	-	Kilovolt



# CHAPTER 1

## INTRODUCTION

### 1.1 Background

One significant element affecting life expectancy is the distribution of the electric field (E-field) along the insulator. A high E-field might cause a discharge activity, which can damage the insulating material and eventually lead to failure [1]. Thus, developing insulating materials to reduce electric fields is crucial for ensuring the safety, reliability, and efficiency of electrical systems. Insulating materials serve as protective barriers, preventing electrical breakdown and mitigating the risk of electric shock, short circuits, and others hazard. Since the 1970s, composite insulators have been used at transmission voltages for a broad range of goals, including cost savings, minimizing the risk of contaminated outages, and resolving vandalism issues.

In the 21st century, polymer nanocomposites have the potential to have a major influence on global economic growth at all levels. The introduction of scanning tunnelling microscopy and scanning probe microscopy in the early 1980s has played a major role in this growth of research in the field of polymer composites [2]. Polymer nanocomposites are composites where a small quantity of nanometer-sized fillers are uniformly distributed within polymers at several weight percentages (wt%) [3]. The development of polymer nanocomposites has been advanced, due to these new materials normally possess greater properties than pure polymers and / or polymer composites because of their new structure[4].

The presence of particle can modify the electric field distribution within the composite, reducing the concentration of electric field lines in specific regions. Several investigations have shown that the existence of the interphase also affects the macroscopic behavior of composites [5]

Tanaka et al.[6] highlight that interfaces play a significant role in the properties of nanocomposites, including dielectric and electrical insulation properties. The multi-

core model proposed is a simplified term for a multi-layered core model to understand various phenomena and properties exhibited by polymer nanocomposites. The model suggests the existence of multiple layers in the interfacial region between the polymer matrix and nano-fillers. This modification helps to prevent localized areas of high stress that could lead to breakdown.

## **1.2 Motivation**

Understanding the need to optimize insulation materials for high voltage applications is essential for designing and maintaining electrical systems. It is motivated to investigate the effect of electric field distribution in polymer composites under varying filler sizes using FEMM 4.2 software. It is expected from this study to contribute in designing materials with superior insulating capabilities, ensuring safety and reliability in electrical systems. The focus is on understanding how variations in filler size influence the electrical performance of insulation materials the electric field within the polymer matrix. It also can be investigated that the addition of nanoparticle enhances the overall properties of the polymer. The nanoscale reinforcement conveys to improve mechanical strength, thermal stability, electrical conductivity, and barrier properties to the composite material. The presence of interphase region which is a layer between the polymer matrix and the nanofiller is asserted to have an impact on the material's properties. Therefore, by using FEMM 4.2 Software, the electric field distribution could be investigated upon different particle size.

## **1.3 Problem Statement**

The performance of materials in terms of electrical properties can be affected by the addition of nanoparticle filler to polymer matrix. However, the tendency of polymer nanocomposites to breakdown is much higher after filled with nanoparticles. Therefore, it is important to investigate the electric field intensity distribution of the polymer nanocomposites performance before it can be used as an alternative insulation in the future. Insulation breakdown is known to be closely related to the electric field produced across the insulator. Partial discharge will take place across a dielectric's impurities when the electric field is sufficiently generated. The dielectric will age and finally break down as a result of repeated partial discharges.

One of the factors that affect the electric field distribution in nanocomposites is the size of fillers particle. By introducing interphase region between it, the material properties will be varied, thus affecting the electric field distribution. However, there are lack of studies on the relationship between electric field distribution with sizing of nanoparticles using software analysis. Therefore, it is proposed to investigate the effect of electric field distribution of polymer nanocomposites under different nanoparticle sizes using FEMM 4.2 software.

#### 1.4 Objectives

The objectives of this project are:

- i. To model the polymer nanocomposites upon different filler size using Finite Element Method Magnetics (FEMM) 4.2 Software.
- ii. To determine the effect of electric field distribution upon different nanoparticle size using Finite Elements Method Magnetics (FEMM) 4.2 software.

#### 1.5 Scope of Work

The scope of work to this study are:

1. A polyethylene (PE) as a host matrix was used in this study.
2. A nanofiller used was Silicon Dioxide ( $\text{SiO}_2$ ). The particle size used were 20nm, 40nm, 60nm, 80nm and 100nm with interphase of 10nm 20nm.
3. Filler loading was fixed at 5wt%.
4. Nanoparticles in polyethylene was distributed homogenously.
5. 2D model in Finite Element Method Magnetics (FEMM) 4.2 software were used to run the simulation.

6. Electric field distribution upon varying nanoparticle sizes was investigated in the simulation.

## 1.6 Thesis Outline

Chapter 1 in this study provides a background of context electric field distribution within polymer nanocomposites. The motivation and the problem statement are defined, objectives of this study and the scope of work are laid out clearly.

Chapter 2 is about literature review that will explore any relevant theories and findings regarding the concept of polymer nanocomposites, structure of polymer, the addition of interphase and modelling and simulation using FEMM 4.2 software.

Chapter 3 which is methodology section highlights the method to achieve the objectives of this study. FEMM 4.2 Software is used to modelling and simulates the electric field distribution on polymer nanocomposites upon different filler sizes. The simulation covers the modelling of spherical silica nanoparticles and the inclusion of an interphase region.

Chapter 4 presents the outcomes of the simulations, including electric field intensity under different filler sizes and the impact on material properties on breakdown strength using FEMM 4.2 Software. There are five different nanofiller sizes (20, 40, 60, 80, 100) nm will be used to investigate the effect of electric field intensity with and inclusion of 10nm and 20nm interphase. The findings are visually represented and organized for clear comprehension.

In this last chapter will conclude the results and discussions from Chapter 5 related to electric field distribution in polymer nanocomposites. It also acknowledges the objectives of the study and provides recommendations for future works.

## CHAPTER 2

### LITERATURE REVIEW

#### 2.1 Introduction

This section provides a comprehensive examination of the interaction between electric fields and nanoparticle sizes in polymer nanocomposites, crucial for understanding the behavior of these advanced materials in electrical engineering applications. Key themes explored include the role of high voltage insulators, the composition and properties of polymer nanocomposites, the influence of nanoparticles on material characteristics, the concept of the interphase region, and theoretical models such as Tanaka's Multi Core Model. Furthermore, this review will examine the simulation of model nanocomposites using advanced software tools like Finite Element Method Magnetics (FEMM) 4.2, shedding light on the practical implications and potential advancements in the field of electrical engineering. It sets the stage for exploring electric field behavior in polymer nanocomposites, leading to new developments in electrical engineering.

#### 2.2 High Voltage Insulator

High voltage insulators are essential components in electrical power transmission systems. Generally, they serve the important role of preventing electrical current from flowing to the ground and insulating conductors from conducting surfaces. These insulators play a crucial role in maintaining the integrity and efficiency of power transmission by preventing loss of electrical energy through heat or arcing to the ground [7], [8], [9].

They are made of materials such as ceramic, glass, or polymers with high electrical resistance and mechanical strength. They are used to support overhead power lines and ensure that electrical energy is safely delivered to consumers without any loss or interruption. In addition to their electrical insulation properties, high voltage

insulators are also designed to withstand various environmental and mechanical stresses.

According to P. Digital [10], these insulators are primarily categorized into pin type, suspension, strain, shackle, and post insulators, each serving specific functions based on the voltage levels and mechanical stresses they encounter. Pin type insulators are commonly used in distribution lines up to 33 kV, mounted on pins on cross-arms of poles. Suspension insulators, composed of porcelain discs linked in series, are utilized for higher voltages above 33 kV, forming strings that provide flexibility and durability. Strain insulators are engineered to handle significant tensile forces in high tension lines, offering robust support under mechanical stress. Shackle insulators, found in low voltage networks, are mounted directly on poles or cross-arms, whereas post insulators, supporting higher voltage lines up to 132 kV and beyond, are essential in substations and switchyards.

The materials used for high voltage insulators include porcelain, glass, and composite materials. Porcelain, known for its excellent mechanical strength and weather resistance, is the most common material, often glazed to prevent dust and moisture accumulation. Glass insulators offer high tensile strength and easy visibility of internal defects, while composite materials, such as polymers with fiberglass cores, provide lightweight, vandal-resistant options with superior hydrophobic properties [7].

### **2.3 Polymer Nanocomposites**

Polymer composites, which consist of a polymer matrix reinforced with particles or reinforcements, often exhibit improved performance compared to pure polymers. The concept of nanocomposite technology was introduced in the early 1990s [11], [12], [13], [14], [15]. Over the last decade, nanocomposites have attracted significant interest in the development of high voltage insulation systems because of their exceptional dielectric properties [11], [16], [17].

The properties of the composites are usually dominated by the particle, depending on their size such as macro-, micro-, or nanoparticles [18]. Polymer nanocomposites are materials in which nanoscale fillers are uniformly distributed

within a polymer matrix in small quantities, typically less than 10% by weight. These fillers, though minimal in amount, significantly enhance the properties of the polymers [3]. With the same nanoparticle loading, nanoparticles have significantly greater reinforcing than micro- and macro-particles. The "nano-effect," or high degree of interaction between nanoparticle and polymer, is what causes this improvement [19].

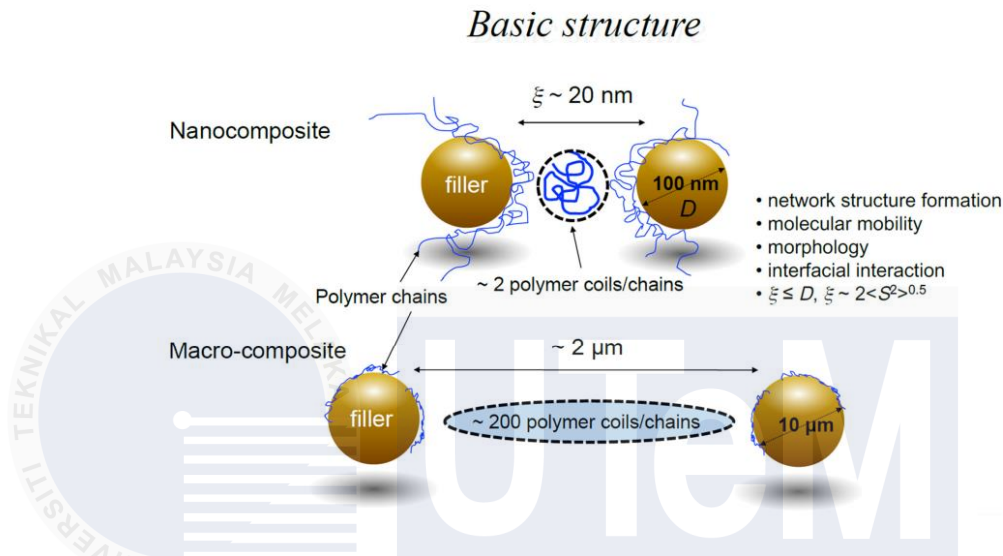


Figure 2.1: Common geometries and reinforcing of particles in nano- and macro-composites [2]

According to Masami Okamoto [2], when the nanoparticle concentration increases, the average value of the particle diameter  $D$  ( $\xi \leq D$ ) is greater than the correlation length between nanoparticle particles  $\xi$ . The  $\xi$  value (about 30 nm) often correlates with the polymer's random coil size. The root-mean-square radius of gyration  $\langle S^2 \rangle^{1/2}$  can be calculated as follows:  $\langle S^2 \rangle^{1/2} = 4.0 \times 10^{-2} M_w^{1/2}$ . This value is about 10 nm.

Polymer nanocomposites can be fabricated using different techniques to achieve a uniform dispersion of nanoparticles of nanoparticles in the polymer matrix. The key challenge lies in preventing nanoparticle aggregation. Researchers have explored preventing nanoparticle aggregation. Researchers have explored various methods, such as chemical reactions, complicated polymerization reactions, or surface modification of fillers [20].

There are four main techniques used for the fabrication of polymer matrix nanocomposites.

The first method is melt compounding, where nanofibers are added to the polymer above its glass transition temperature. The shear stress induced in compounding, where nanofibers are added to the polymer above its glass transition temperature. The shear stress induced in the polymer melt breaks down the nanofiller aggregates, promoting homogeneous dispersion in the polymer melt breaks down the nanofiller aggregates, promoting homogeneous dispersion in the polymer matrix [21].

The second method is the solvent method, which involves dispersing nanoparticles in a solvent and dissolving the polymer in a co-solvent. The resulting nanocomposites are obtained by recovering the polymer from the solvent, either through solvent evaporation or solvent coagulation[21].

The third method is in situ polymerization, which entails the formation of the polymer in the presence of nanofillers. This method allows for the simultaneous synthesis of the polymer matrix and dispersion of nanoparticles [21].

Finally, the fourth method is intercalation, where nanofillers are dispersed between the polymer chains or layers using solvents. This technique aims to achieve a uniform distribution of nanoparticles [21].

The most used methods for manufacturing polymer nanocomposites are in situ polymerization and melt blending. Even the incorporation of a small percentage of nanoparticles into the polymer matrix significantly enhances the electrical, mechanical, physical, and chemical properties of the nanocomposites [11], [22], [23]. This advancement in nanotechnology has led to notable improvements in electrical insulation systems [11].

These polymer matrix nanocomposites can be further processed using conventional manufacturing techniques like injection molding, calendaring intercalation, where nanofillers are dispersed between the polymer chains or layers using solvents. This technique aims to achieve a uniform distribution of nanoparticles [20].



## 2.4 Polymer

A polymer is a type of substance, whether naturally occurring or artificially created, characterized by the presence of highly extensive molecules known as macromolecules. These macromolecules are comprised of repeated and interconnected simpler chemical units called monomers [24].

According to the International Union of Pure and Applied Chemistry [25], “A polymer is a substance composed of molecules characterized by the multiple repetitions of one or more species of atoms or groups of atoms (constitutional repeating units) linked to each other in amounts sufficient to provide a set of properties that do not vary markedly with the addition of one or a few of the constitutional repeating units.” Polymers can be broadly categorized into the following four types [26]:

a. Thermoset – A polymer with cross-links that prevent it from melting, as seen in rubbers and tires.

b. Thermoplastic – A polymer with cross-links that has the ability to melt, as seen in plastics.

c. Elastomer – A polymer that can deform, stretching and then returning to its original form; also referred to as thermoset polymers.

d. Thermoplastic elastomer – An elastic polymer capable of melting, for instance, in footwear and shoe soles.

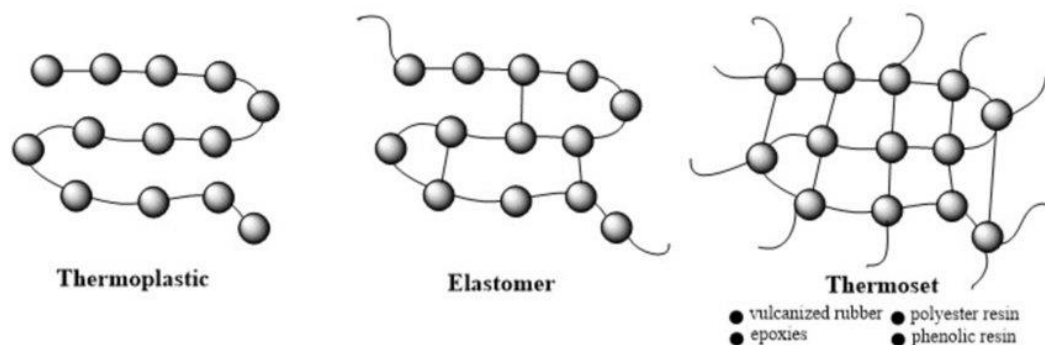


Figure 2.2: Formation of thermoplastic, elastomer and thermoset [27]

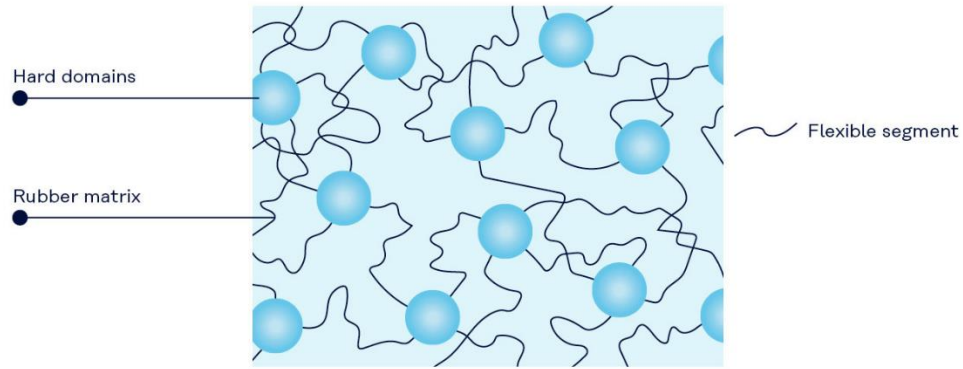


Figure 2.3: Formation of thermoplastic elastomer [28]

## 2.5 Nanoparticle / Nanofiller

Nanofillers / nanoparticles play a crucial role in enhancing the properties of polymer nanocomposites. These materials, with at least one dimension in the nanoscale range (10–100 nm), are dispersed homogeneously within the polymer matrix [1]. The incorporation of nano nanoparticle s aims to maximize the "nano-effect" derived from the nanoparticles while minimizing the disadvantages of the polymer. Nano nanoparticles can take various forms, such as nanosheets, nanotubes, nanofibrils, and quantum dots, and are utilized to fabricate polymer nanocomposites with tunable mechanical, thermal, electrical, magnetic, and optical properties [29].

The high aspect ratio of nanomaterials, due to their large surface area for a fixed volume, imparts superior properties to the polymer nanocomposites, leading to significant improvements in performance [30]. Nanoparticles used in electrical insulating nanocomposites can be categorized into four main groups, each contributing unique properties that enhance the performance of the insulation materials:

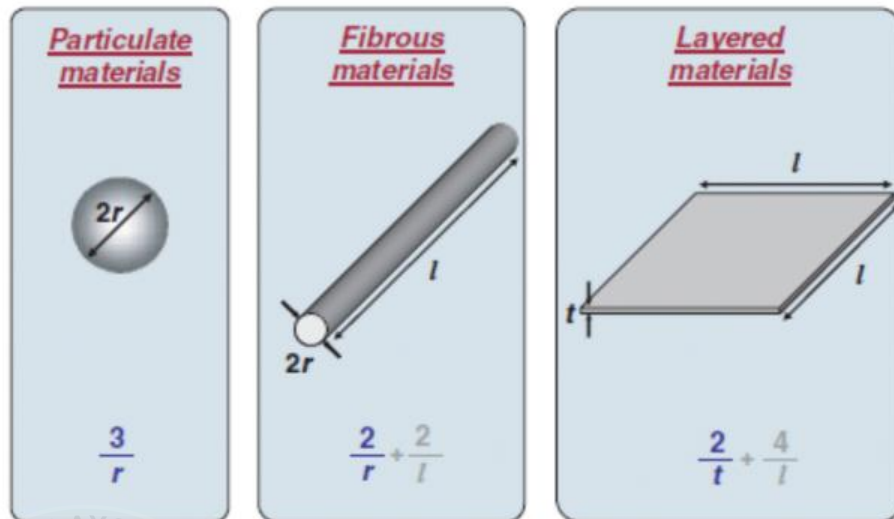
**Metal Oxides:** This category includes nanoparticles like titanium dioxide ( $\text{TiO}_2$ ), zinc oxide ( $\text{ZnO}$ ), and aluminum oxide ( $\text{Al}_2\text{O}_3$ ). These nanoparticles are valued for their high dielectric strength and thermal stability. Incorporating them into polymer matrices improves the dielectric and thermal properties, making the composites more effective as insulating materials.

Carbon-Based Nanomaterials: Examples of these include carbon nanotubes (CNTs) and graphene. They are renowned for their excellent electrical conductivity and mechanical strength. When added to polymers, they significantly enhance the electrical and mechanical performance of the nanocomposites, which is essential for various electrical insulation applications.

Nanoclays: Nanoclay particles, such as montmorillonite, are used to enhance the mechanical and barrier properties of polymer nanocomposites. They also improve thermal stability and flame retardancy, which are critical characteristics for materials used in electrical insulation.

Polymer-Based Nanoparticles: This group includes organic nanoparticles like dendrimers and hyperbranched polymers. These nanoparticles improve the compatibility between the polymer matrix and other nanoparticles, ensuring better dispersion and enhanced overall properties of the composite.

According to Masami Okamoto [2], when dealing with particles, platelets, or fibers, the relationship between the surface area per unit volume and the material's diameter  $D$  is inversely proportional. The ratio of surface area to volume ( $R$ ) is expressed as  $6/D$ . As the diameter decreases, the surface area per unit volume increases. Figure 2 illustrates various particle geometries and their corresponding values of  $R$  [2]. In the case of fiber and layered (platelet) materials, the impact of the first term in the equation is significant, whereas the second term ( $2/l$  and  $4/l$ ) has a negligible effect in comparison. Therefore, a reduction in the diameter from the micrometer to nanometer range results in a substantial alteration of  $R$  by three orders of magnitude[2]. Nanoparticles, nanotubes, nanofibers, fullerenes, and nanowires are examples of common nano- nanoparticles that are being studied. These materials are categorized into three groups based on their geometries, such as one-, two-, or three-dimensional nanoscale materials, as Figure 2 illustrates[31],[32]:



- Nano-silica
- Nano-silicon carbide
- Nano-zinc oxide
- Nano-silver
- Carbon black
- POSS
- Others ( $n$ -BaTiO<sub>3</sub>,  $n$ -CaCO<sub>3</sub>)
- Carbon nanofibers
- Carbon nanotubes
- Halloysite nanotubes
- Nickel nanostrand (NiNs)
- Layered silicate (Montmorillonite)
- Layered double hydroxide (LDHs)
- Layered titanate
- Nanographene platelets

Figure 2.4: Common particle reinforcements/geometries and their respective surface area-to-volume ratios R [2]

## 2.6 Interphase

In nanocomposites material, the term “interphase” refers as a layer or region between nano nanoparticles and the matrix material. Interphase plays a crucial role to enhance properties, such as improved strength, stiffness and thermal stability. Researchers often focus on adapting the interphase properties through surface modifications of nanoparticles, choosing appropriate matrix materials, or using coupling agents to improve the compatibility between the nano nanoparticles and the matrix.

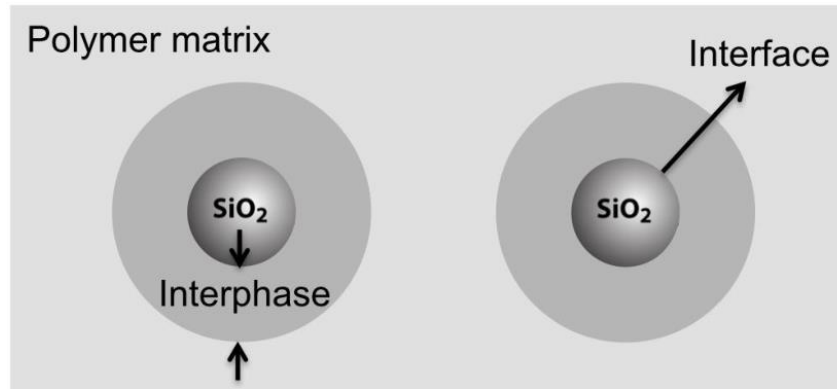


Figure 2.5: Interphase concept in polymer nanocomposites [33]

According to Huang et. al [1], the interphase is a region where the chain dynamics differ from those of the bulk, and its characteristics are different from the bulk polymer. The thickness of the interphase depends on various factors, including the equilibration time, the molecular weight of the polymer chain, and the adsorbed chain conformation. In nanocomposites, the interface area between the nanofillers and polymers drastically increases with the reduction of at least one characteristic size of the fillers to a nanometer scale. This amplified interface area enhances the interactions between the nanofillers and polymer chains, leading to improved macroscopic material properties.

The size effect of the interphase plays an important role in polymer nanocomposites. As demonstrated both experimentally and through simulations, the interparticle separation distance ( $d$ ) and thickness of the interphase ( $h$ ) determine the degree of influence of the interphase. When the interphases on adjacent nanoparticles overlap ( $d/h \leq 1$ ), the interphase effect is most significant [1].

Studies, such as those conducted by Priestley et al., have used advanced techniques like transmission electron microscopy (TEM) to directly visualize the interfacial adsorption layer around nanoparticles. By investigating the correlation between the interfacial layers' structures and the glass transition temperature ( $T_g$ ), researchers have gained insights into how the interphase influences the overall behavior of nanocomposites [1], [34].

Senses et al. used X-ray photon correlation spectroscopy to investigate how the nanoparticle relaxation behavior changed with nanoparticle fraction (interparticle separation distance) in polyethylene oxide) nanocomposites. They observed that at a nanoparticle fraction of 25%, where  $d/2R_g \approx 1$ , the nanoparticle relaxation became extremely slow and exhibited hyper diffusive behavior. This indicates strong polymer bridging between nanoparticles forming a network structure [1], [35].

Furthermore, research by Starr et al. has shed light on the impact of interparticle separation within the interphase on chain relaxation in polymer nanocomposites. Understanding and controlling the interphase are essential for tailoring the material properties of nanocomposites. By adjusting the thickness and structure of the interphase, it is possible to optimize the performance of these advanced materials [1], [36].

Overall, the interphase in polymer nanocomposites is essential for facilitating enhanced interactions between nanofillers and polymer chains, leading to improved material properties.

## 2.7 Tanaka's Multi Core Model

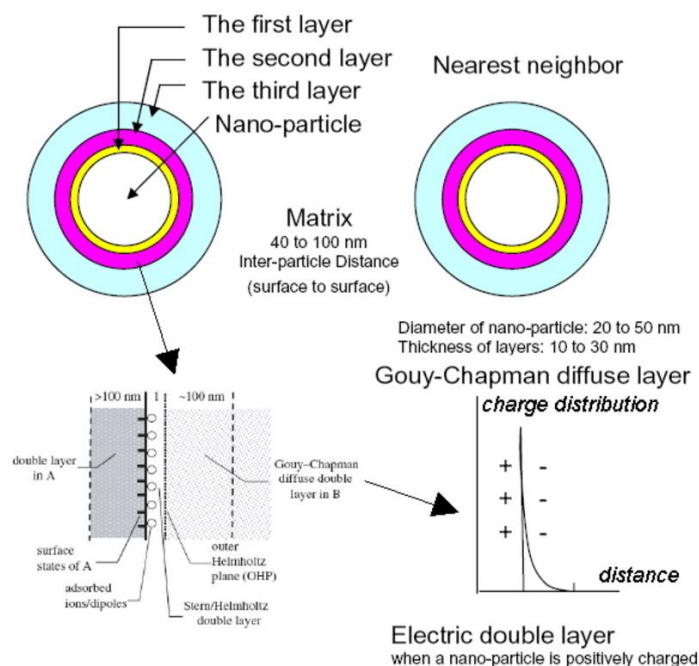


Figure 2.6: Tanaka's Multi Core Model [37]

The multi-core model proposed by Tanaka et al. is a hypothesis to understand the behavior and properties exhibited by polymer nanocomposite dielectrics. It is a simplified term for a multi-layered core model that describes the fine structures of what are known as "interaction zones" between the polymer matrix and nano-fillers. The interfacial layer between the matrix and fillers consists of several layers, including a bonded layer, a bound layer, and a loose layer.

The multi-core model for nano-particle-polymer interfaces consists of three layers: the bonded layer, the bound layer, and the loose layer.

**Bonded Layer (First Layer):** This layer is tightly bonded to both the inorganic particles (nano-fillers) and the polymer matrix through coupling agents like silane. It serves as a transition layer between the inorganic and organic substances.

**Bound Layer (Second Layer):** The bound layer is an interfacial region where the polymer chains strongly bind and/or interact with both the bonded layer and the surface of the inorganic particle. Its thickness usually ranges from 2 to 9 nm.

**Loose Layer (Third Layer):** The loose layer is a less tightly bound layer where the interaction between the polymer chains and the inorganic particle surface is weaker.

In addition to these layers, the Gouy-Chapman diffuse layer is superimposed on the interfacial layer. This layer, with a Debye shielding length ranging from several tens to 100 nm, creates a far-field effect. This far-field effect allows nanoparticles to interact electrically with their nearest neighbors, potentially resulting in a collaborative effect. The presence of the Gouy-Chapman diffuse layer and its interaction with neighboring particles is a key aspect of the multi-core model for understanding the behavior and properties of polymer nanocomposites.

## 2.8 Literature Review on The Simulation of Model Nanocomposites

Modeling nanocomposites is essential for advancing material science and enables researchers to predict the properties and behaviors of nanocomposites under various conditions, saving time and resources compared to experimental trials. The performance of high voltage insulators hinges upon a crucial factor, which is the distribution of the electric field within the material. According to K.Y. Lau et. al [37], FEMM software is commonly used for electric field analysis. It can be used to solve electrostatic problems and analyze electric field distribution. In this study, the size of particles (nano vs micro) affects the electric field intensity within polymer composites.

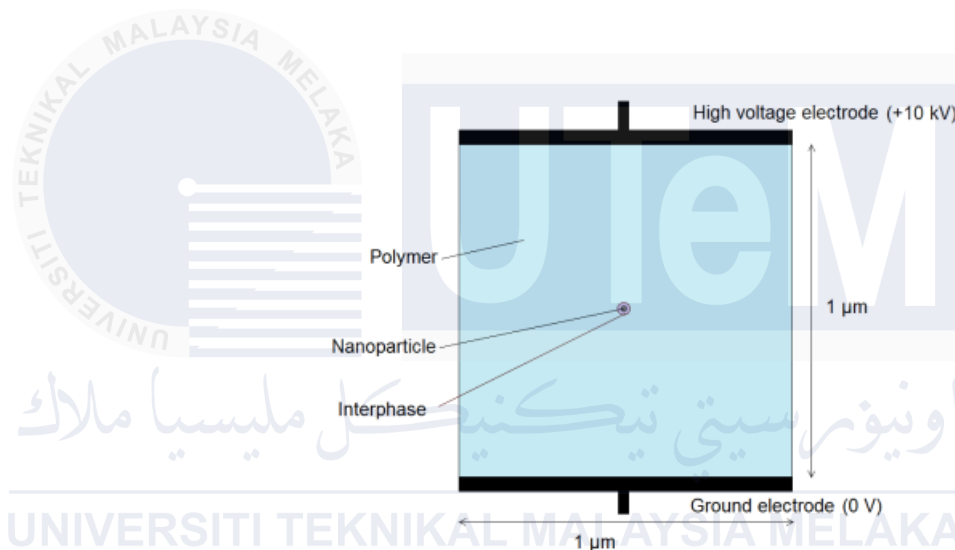


Figure 2.7: A 2D unit cell model ( $1 \mu\text{m} \times 1 \mu\text{m}$ ) of a nanocomposite consisting of a polymer, a nanoparticle, and an interphase, positioned between a high voltage electrode and a ground electrode [37]

It modelled the effects of a nanometer-sized particle and its interphase on the electric field distribution within polymer nanocomposites. Parameters varied include the nanoparticle size (micro vs nano), permittivity of the nanoparticle and interphase, to determine their effects on the electric field. Results showed that a smaller nanoparticle size leads to less electric field distortion compared to a microparticle, indicating benefits of nanocomposites. Varying nanoparticle and interphase permittivity can significantly enhance or reduce electric field intensity surrounding them. While for the unfilled polymer, it was found that the electric field remained constant at approximately  $1.00 \times 10^4 \text{ kV mm}^{-1}$ . Combining nanoparticles and



polymer with appropriate permittivity values can enhance or reduce electric field intensity, which has implications for dielectric breakdown strength and performance.

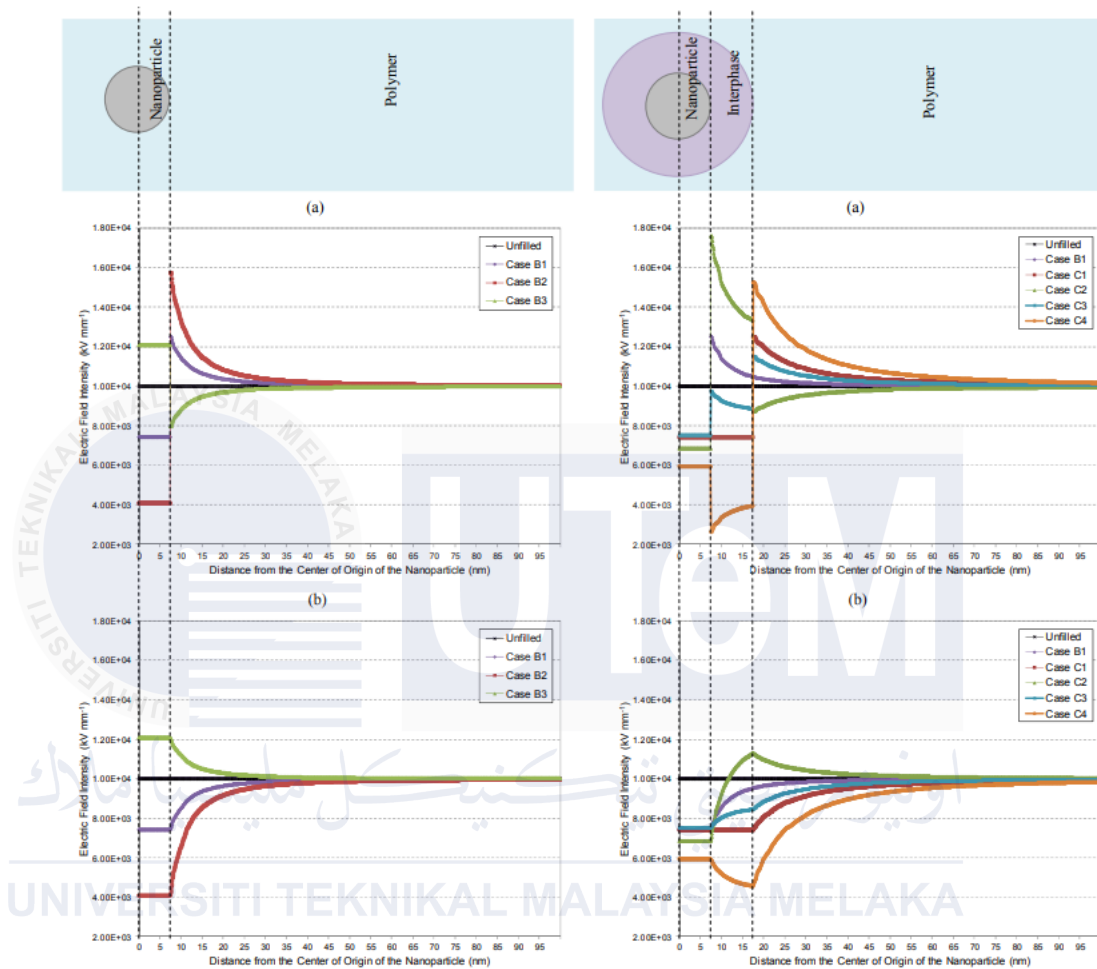


Figure 2.8: Effect of (a) nanoparticle (without interphase) on the electric field intensity plots along the (b) 90° vertical line and (c) 0° horizontal line, originating from the center of the nanoparticle and extending into the polymer region [37]

Ziming Cai et. al [38] introduces a quantified method based on the Clark-Evans test to describe the distribution of ceramic nanoparticles. They use finite element method and phase field method in COMSOL Multiphysics 5.2a to analyze the effects of nanoparticle distribution on the dielectric properties and breakdown behavior of the nanocomposites. The study finds that a non-uniform distribution of ceramic nanoparticles leads to a concentration of the local electric field, slightly enhancing the dielectric response but significantly reducing the breakdown strength. It also explores the size effect of ceramic particles on the breakdown strength of nanocomposites by

calculating the breakdown strength for three types of well-distributed nanoparticles with different diameters. The results show that larger ceramic particles decrease the breakdown strength.

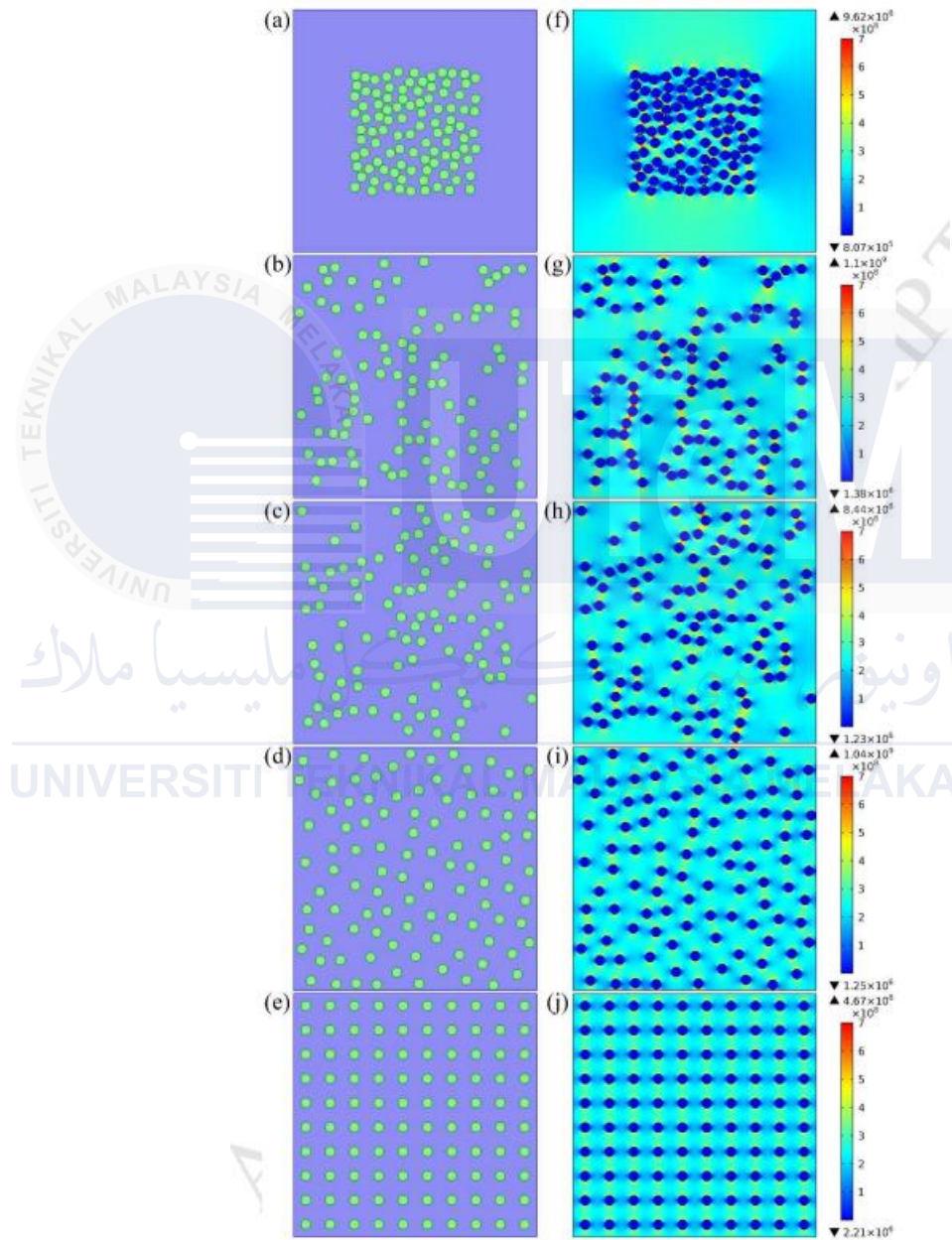


Figure 2.9: Five different random distributions of ceramic particles in polymer matrix from (a) to (e); (f) to (j) is the distribution of electric field strength corresponding to each random distribution [38]

Figure 2.9 is a series of illustrations that depict five different random distributions of ceramic particles within a polymer matrix, labeled from (a) to (e). These distributions are part of the study's investigation into how the arrangement of ceramic nanoparticles affects the dielectric response and breakdown strength of polymer-ceramic nanocomposites.

Each subfigure (a) through (e) represents a unique case of particle distribution, with the ceramic particles shown as circular domains within a square region that symbolizes the polymer matrix. The distributions vary from less uniform to more uniform, and the study uses a quantified method based on the Clark-Evans test to evaluate the uniformity of these distributions.

Additionally, for each distribution case, there is a corresponding subfigure (f) through (j) that shows the distribution of electric field strength (in the unit V/m) under an applied electric field of 200 MV/m. These subfigures illustrate how the electric field is concentrated around the ceramic particles and how this concentration varies with the distribution of the particles.

The purpose of Figure 2.9 is to visually represent the different scenarios of nanoparticle distribution and to show the resulting electric field patterns, which are crucial for understanding the dielectric behavior and breakdown mechanisms in the nanocomposites. The figure serves as a visual aid to complement the quantitative analysis presented in the manuscript.

In addition, Lau K et. al [39] aims to understand the dielectric properties of nanocomposites, which are promising materials for high voltage electrical insulation due to their potential to enhance conventional insulation systems. The study proposes various interphase models to explain the interaction zone between the nanofiller and the polymer, which influences the dielectric behaviour of nanocomposites.

Experimental work involved the preparation of nanocomposite samples with different weight percentages of nanosilica and characterization through breakdown testing. The results showed that adding nanosilica reduced the DC breakdown strength,

with the effect being more pronounced at higher nanofiller contents. AC breakdown strength, however, showed an insignificant variation with the addition of nanosilica.

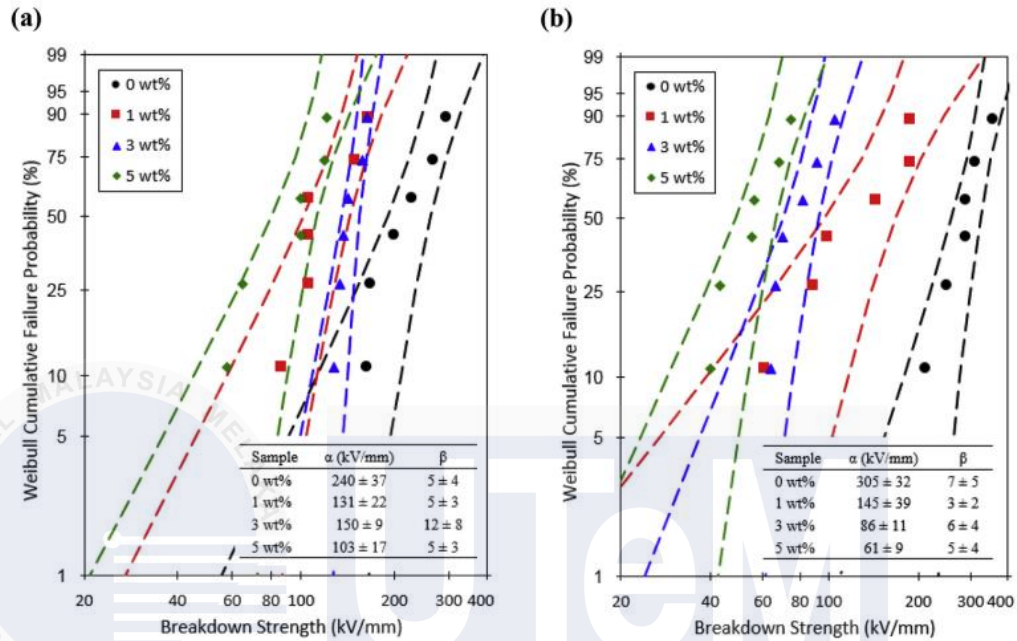


Figure 2.10: Weibull plots comparing the DC breakdown strength of (a) LDPE, (b) HDPE containing 0 wt%, 1 wt%, 3 wt%, and 5 wt% of nanosilica [39]

Figure 2.10 (a) illustrates Weibull plots comparing the DC breakdown strength of LDPE with varying nanosilica content: 0 wt%, 1 wt%, 3 wt%, and 5 wt%. The unfilled LDPE exhibited a DC breakdown strength of 240 kV/mm. With the addition of 1 wt% nanosilica, the DC breakdown strength decreased to 131 kV/mm. When the nanosilica content increased to 3 wt%, the breakdown strength slightly improved to 150 kV/mm. However, considering the uncertainties inherent in Weibull analysis, the difference in breakdown strength between the 1 wt% and 3 wt% nanosilica-filled LDPE is minimal. The LDPE containing 5 wt% nanosilica had the lowest DC breakdown strength of all samples, at 103 kV/mm. To validate these findings, a similar experiment was conducted using HDPE instead of LDPE, which revealed a comparable breakdown trend in Figure 2.10 (b) [39].

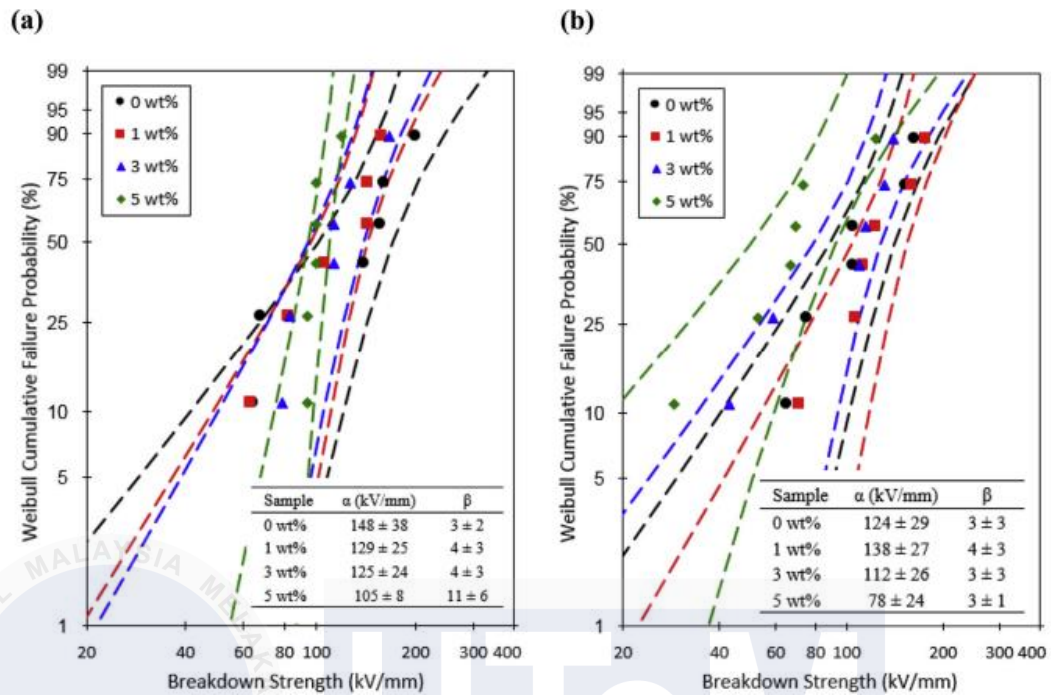


Figure 2.11: Weibull plots comparing the AC breakdown strength of (a) LDPE, (b) HDPE containing 0 wt%, 1 wt%, 3 wt%, and 5 wt% of nanosilica [39]

Figure 2.11 (a) shows Weibull plots comparing the AC breakdown strength of LDPE with different concentrations of nanosilica: 0 wt%, 1 wt%, 3 wt%, and 5 wt%. The AC breakdown strength of unfilled LDPE was measured at 148 kV/mm. When 1 wt% of nanosilica was added, the AC breakdown strength decreased to 129 kV/mm. Increasing the nanosilica content to 3 wt% resulted in a slight further decrease in breakdown strength to 125 kV/mm. However, given the uncertainties in Weibull analysis, the differences in AC breakdown strength among LDPE with 0 wt%, 1 wt%, and 3 wt% of nanosilica are minimal. The LDPE sample with 5 wt% nanosilica had the lowest AC breakdown strength at 105 kV/mm. To verify these results, a similar experiment was conducted using HDPE instead of LDPE, which showed a comparable breakdown trend in Figure 2.11 (b).

Finite Element Method Magnetics (FEMM) 4.2 software was used to simulate the electric field distribution in proposed nanocomposite models. The simulations revealed that the permittivity of the interphase significantly affects the electric field distribution. When the interphase permittivity is between that of the nanoparticle and the polymer, the electric field distortion is minimized, potentially improving

breakdown performance. Conversely, a large mismatch in permittivity can lead to electric field distortion and reduced breakdown strength.

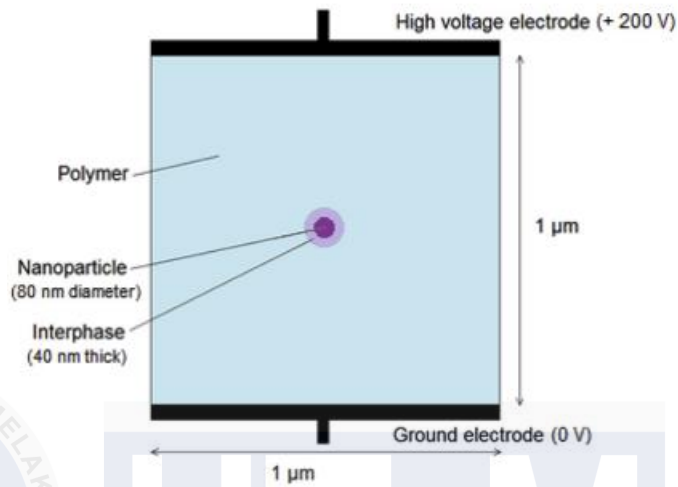


Figure 2.12: A 2D unit cell model (1  $\mu\text{m} \times 1 \mu\text{m}$ ) of a nanocomposite consisting of a polymer, a nanoparticle, and an interphase, situated between a high voltage electrode and a ground electrode[39]

Table 2.1: Models and parameter [39]

Model	Permittivity			Remarks
	Polymer, $\epsilon_1$	Nanoparticle, $\epsilon_2$	Interphase, $\epsilon_3$	
Polymer Model	Fixed: 2.3	–	–	No nanoparticle
Nano Model I	Fixed: 2.3	Fixed: 3.9	Varied: 1.5, 3.0, or 9.0	Single nanoparticle
Nano Model II	Fixed: 2.3	Fixed: 3.9	Varied: 1.5, 3.0, or 9.0	Interparticle distance: 0 nm (overlapped interphase)
Nano Model III	Fixed: 2.3	Fixed: 3.9	Varied: 1.5, 3.0, or 9.0	Interparticle distance: 40 nm (overlapped interphase)
Nano Model IV	Fixed: 2.3	Fixed: 3.9	Varied: 1.5, 3.0, or 9.0	Interparticle distance: 80 nm (non-overlapped interphase)
Nano Model V	Fixed: 2.3	Fixed: 3.9	Varied: 1.5, 3.0, or 9.0	Interparticle distance: 120 nm (non-overlapped interphase)
Nano Model VI	Fixed: 2.3	Fixed: 3.9	Varied: 1.5, 3.0, or 9.0	Interparticle distance: 240 nm (non-overlapped interphase)
Particle Size Model	Fixed: 2.3	Fixed: 3.9	Fixed: 3.0	Single nanoparticle with varied sizes: 80 nm, 70 nm, or 10 nm

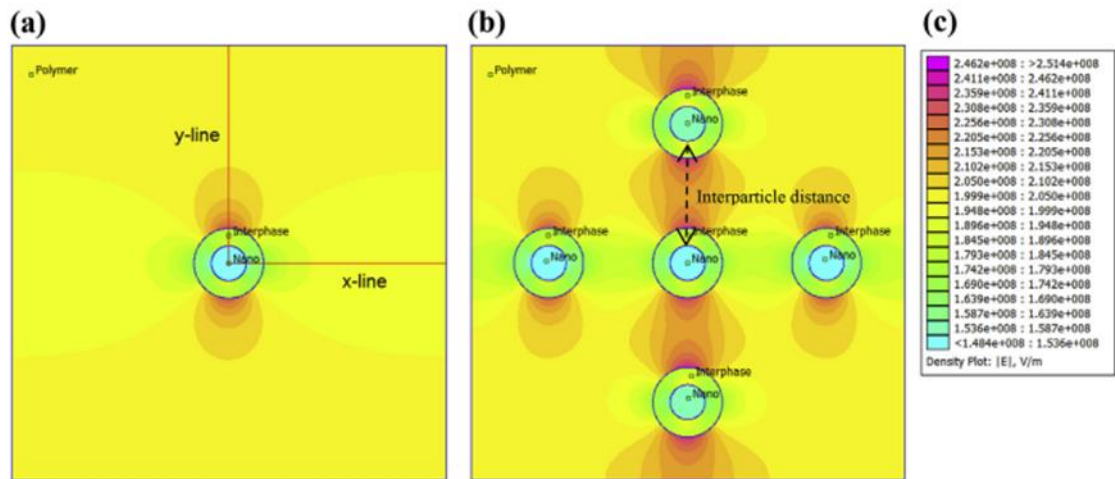


Figure 2.13(a): Illustration of a nanocomposite with an interphase. The vertical (y-line) and horizontal (x-line) lines indicate the locations where electric field intensity data were collected for Nano Model I. (b) Depiction of a nanocomposite with nanoparticles and interphases, with the nanoparticles separated by a defined interparticle distance [39]

The study also found that the electric field distribution is less distorted when nanoparticles are separated by greater distances, suggesting that nanocomposites with lower nanofiller contents may have better breakdown performance. Additionally, smaller nanoparticles with a smaller interphase thickness lead to less electric field distortion compared to larger nanoparticles.

The study provides insights into the DC and AC breakdown behaviors of polyethylene/silica nanocomposites, highlighting the importance of the interphase permittivity and nanoparticle distribution in determining the electric field distribution and breakdown strength of these materials. The findings contribute to the understanding of nanocomposite dielectrics and may guide the development of high-performance electrical insulation materials.

In conclusion, incorporating nanoparticles into polymer matrices to form nanocomposites offers significant advantages for electrical engineering applications. These nanocomposites exhibit superior properties compared to pure polymers, including enhanced mechanical strength, thermal stability, electrical insulation, and flame retardancy. The interaction between electric fields and nanoparticle sizes plays a crucial role in optimizing these properties, with nanoparticle size and distribution

influencing the material's performance under high voltage conditions. The use of advanced simulation tools like Finite Element Method Magnetics (FEMM) 4.2 enables efficient exploration of these interactions and the development of high-performance nanocomposites tailored to specific applications. One key benefit of using FEMM 4.2 over experimental methods is its cost-effectiveness and time efficiency, allowing researchers to explore a wide range of parameters and scenarios in a controlled virtual environment without the need for costly and time-consuming physical experiments. Overall, the inclusion of nanoparticles into polymer matrices shows great promise for advancing electrical insulation systems, leading to more efficient and reliable electrical engineering solutions.





## CHAPTER 3

### METHODOLOGY

#### 3.1 Introduction

This chapter discusses the methodology that is used to achieve the objectives of the project. This introduction to the methodology section provides an overview of the approach taken to conduct the research and outlines the steps involved in utilizing the Finite Element Method Magnetics (FEMM) 4.2 software for simulations. It begins with the creation of composite polymer models featuring different nanoparticle sizes, recognizing the essential role of nanoparticle materials in determining overall electrical properties. Notably, the interphase, the region between the nanoparticle and polymer matrix, will be carefully considered for its potential influence on electrical behavior.

#### 3.2 Project Flow

To provide a clear and structured representation of the project's methodology, the following flowchart has been developed. This visual tool is designed to illustrate the sequential steps, decision points, and key processes involved in investigating the influence of nanoparticle sizes on electric field characteristics within composite polymers. This flowchart aims to enhance understanding, facilitate communication, and serve as a comprehensive guide to the project's workflow and methodology. Figure 3.1 shows the flowchart of this project [19]:

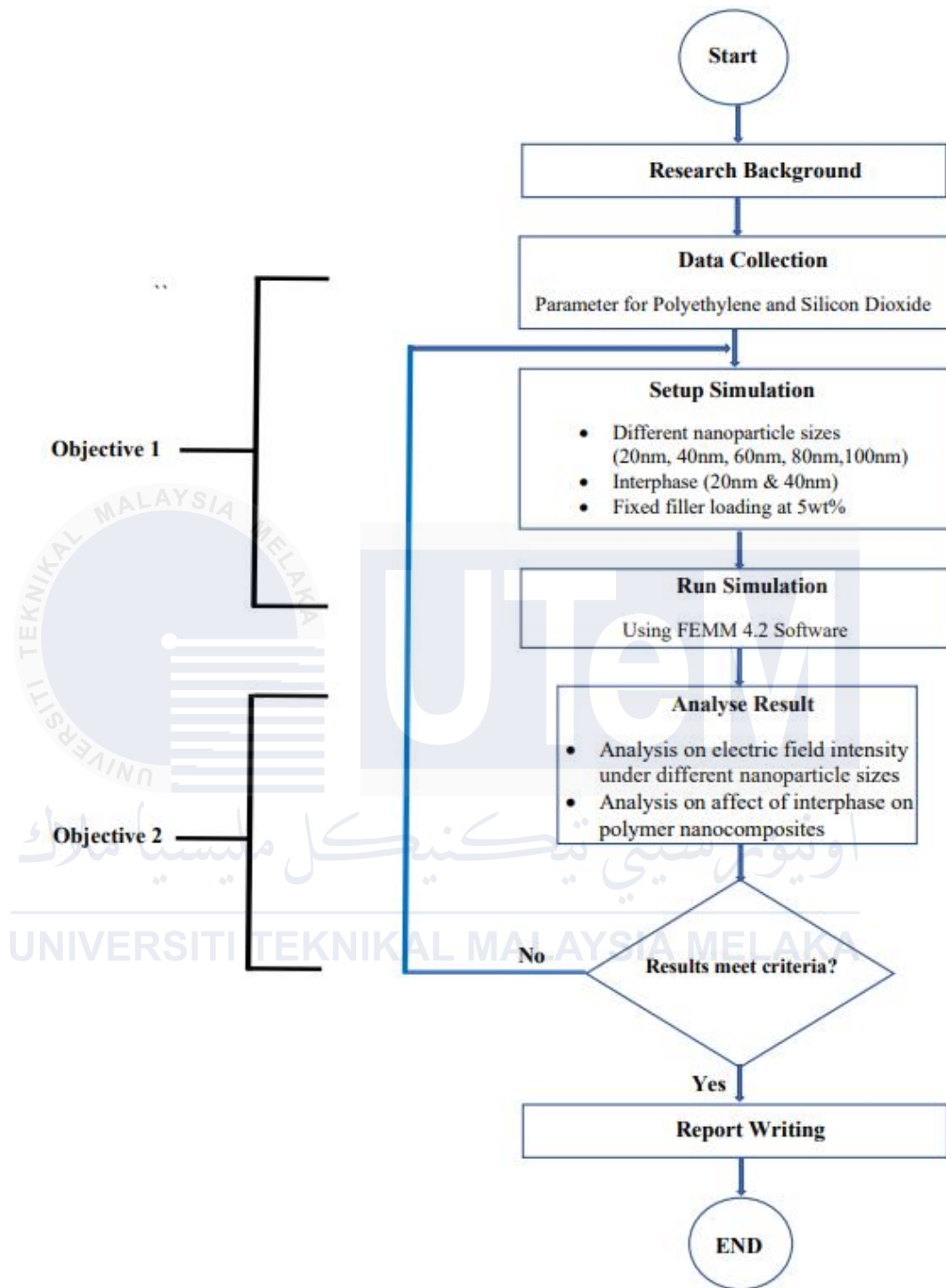


Figure 3.1: Flowchart of the project

### 3.3 K-Chart

Figure 3.2 shows the overall project. K-Chart provides a simple way to follow the progress of a research project while at the same time maintaining a good overview of the whole project's scope.

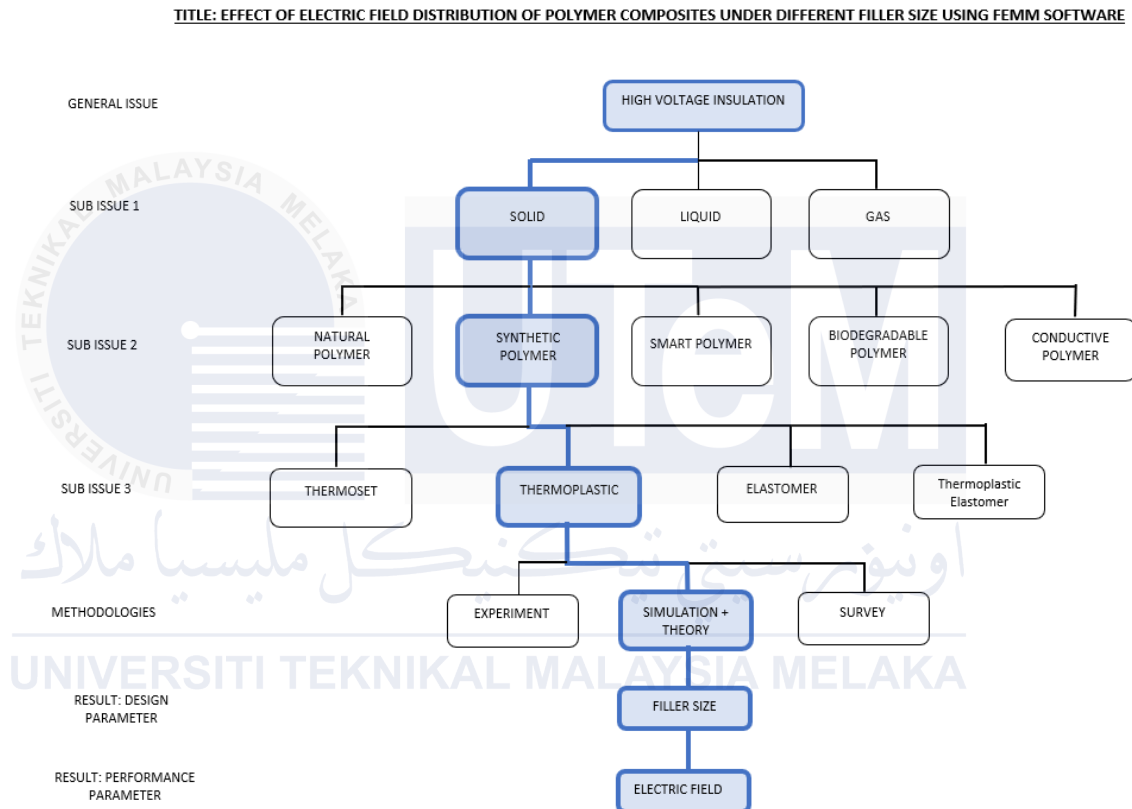


Figure 3.2: K-Chart of the project

### 3.4 Finite Element Method Magnetics (FEMM) 4.2 Software

FEMM 4.2 is an open-source software, which users can modify and share it without restriction. This is a package of program designed to solve low-frequency electromagnetic problems on two-dimensional planar and axisymmetric domains [37]. Currently, the programmer covers linear electrostatic problems, steady-state heat flow problems, linear / nonlinear magnetostatic problems, and linear/nonlinear time harmonic magnetic problems [18].

Finite element analysis is a strong and accurate method in complex geometrical modelling which provides solutions in a variety field of engineering[37]. In this case, the characteristics of an insulation materials in high voltage insulation relies on on how resistant it is to voltage or how strong the electric field is [19]. The degradation or breakdown of the insulating material is often caused by high voltage and high electric field intensity within the material. To create insulating materials with the ideal electric field intensity, electric field analysis is applied [17].

According to David Meeker [18], FEMM 4.2 is divided into three parts: Interactive shell (femm.exe), triangle.exe and solvers. This program is a Multiple Document Interface pre-processor and a post-processor for the various types of problems solved by FEMM. The pre-processing is used for drawing the geometry problems defining materials and boundary conditions. While the electrostatics post processing is used to view solutions generated by the belsolve solver. The vital part of the finite element process is the triangle.exe which breaks down the solution region into a large number of triangles.

### 3.5 Polymer Nanocomposites Modelling

For simulation purpose, the parameters of properties of the materials were assumed as in Table 3.13. To simulate homogeneous dispersion, the position and distance between adjacent of particles were distribute in uniform.

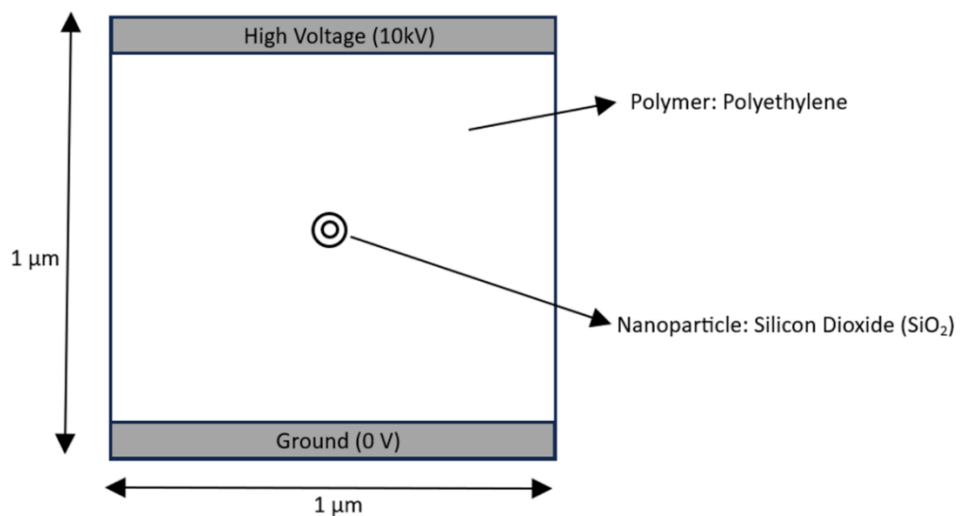


Figure 3.3: A two-dimensional polymer slab with dimension of  $1\ \mu\text{m} \times 1\ \mu\text{m}$

Using FEMM 4.2's electrostatic module, a polymer nanocomposite consists of a polymer matrix, nanoparticles, and an interphase area was modelled. As seen in Figure 3.9, the basic polymer slab measuring 1  $\mu\text{m}$  by 1  $\mu\text{m}$  was positioned between a ground potential and a high voltage potential of 10 kV. The simulation only uses this high voltage potential value; it is not applicable to experimental work since the nanocomposite sample's thickness cannot withstand such a high voltage. In this model, polyethylene was used as the polymer and silicon dioxide ( $\text{SiO}_2$ ) as nanoparticle. The polymer matrix and nanoparticles have fixed permittivity values of 2.3 and 3.9 respectively. The following assumptions for the nanocomposites for ease the simulation are made:

- i. The model of nanoparticle was spherical shape and dispersed homogenously.
- ii. The model contained interphase of 10nm and 20nm.
- iii. The electric field intensity was mainly affected by the variation in nanoparticle sizing.
- iv. The electric field intensity was not considerably affected by space charge and temperature effects.

Table 3.1: Modelling parameters of the materials

Filler Size (nm)	Polymer - Filler	Interphase Size	Permittivity
20	PE – $\text{SiO}_2$	10nm	Polymer: 2.3 Filler: 3.9 Interphase: 2.0
40			
60		20nm	
80			
100			

### 3.6 Finite Element Method Magnetics (FEMM) 4.2 Software Setting

When FEMM 4.2 is opened from the Start menu, the window shown in Figure 3.3 of FEMM 4.2 displayed.



Figure 3.4: Finite Element Method Magnetic (FEMM) 4.2 display

A new file is chosen and to solve electrostatics problem, electrostatics problem is created for electric field analysis purposes in Figure 3.5. This section is pre-processing which is used for drawing the geometry problems defining materials and boundary conditions.

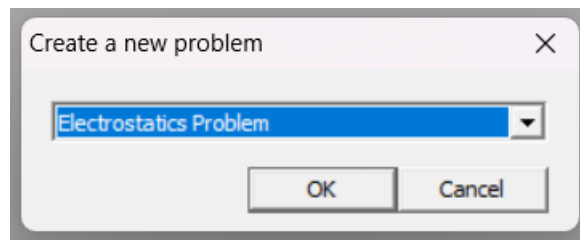
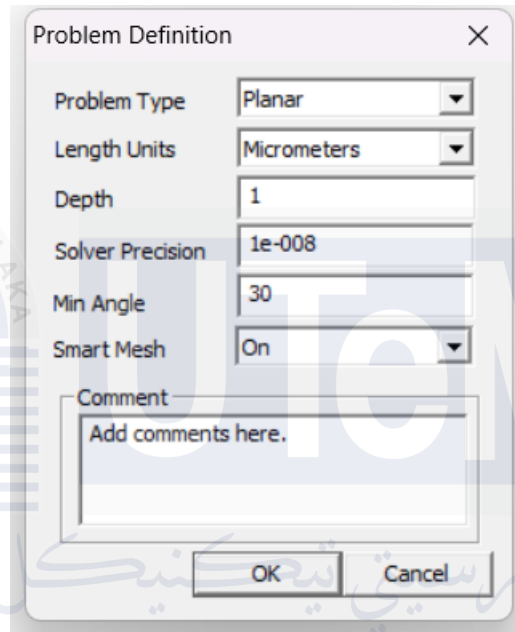


Figure 3.5: Create New Problem Dialog

Then Figure 3.6 shows the problem definition dialog. The problem type is set to planar which simplifies the analysis of electromagnetic fields within a two-dimensional (2D) plane and length units are set to micrometers. Next, the solver

precision is set to default i.e 10-8 to determine when the solution has reached a sufficiently accurate result during the simulation process. The min angle edit box is used as a constraint in the triangle meshing program. Triangle adds points to the mesh to ensure that no angles smaller than the specified angle occur and it is set to default of 30.



UNIVERSITI TEKNIKAL MALAYSIA MELAKA  
Figure 3.6: Problem Definition dialog

There are five (5) operations for drawing the problems geometry in FEMM listed as nodes, segments, arc segments, block labels and group of objects of tool bar buttons as shown in Figure 3.7 below.



Figure 3.7: tool bar buttons

To define the properties of materials used, we could check it on materials library shown in Figure 3.8. If the materials we used did not appear, materials block property dialog is chosen. The Block Property dialog box is used to specify the

properties to be associated with block labels. The properties specified in this dialog have to do with the material or boundary of which the block is composed.

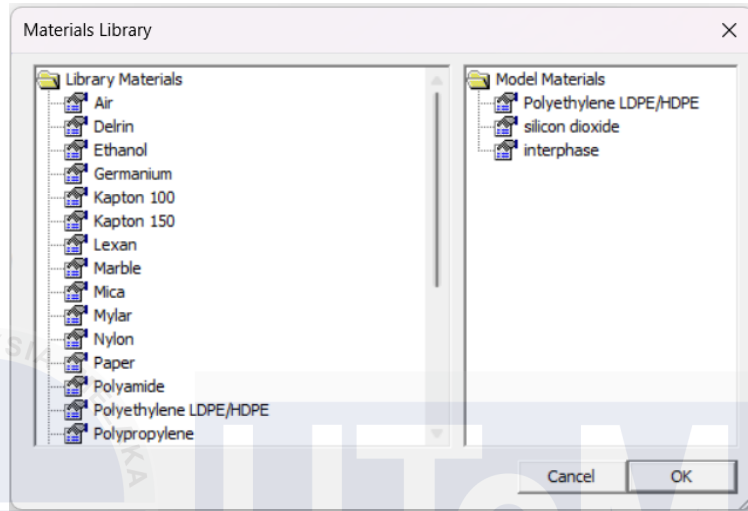


Figure 3.8: Materials Library dialog

When a new material or boundary property is added or an existing property modified, the Block Property dialog pictured in Figure 3.9 appears. The permittivity and the volume charge density also can be specified or modified in the properties dialog.

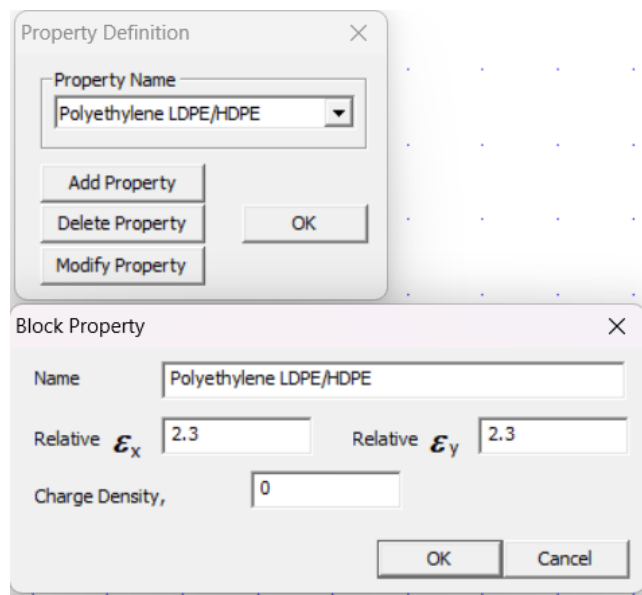


Figure 3.9: Block Property dialog for materials



Figure 3.10 shows the block property for boundaries. In this block, the value of high voltage (10kV) the ground (0V) was added.

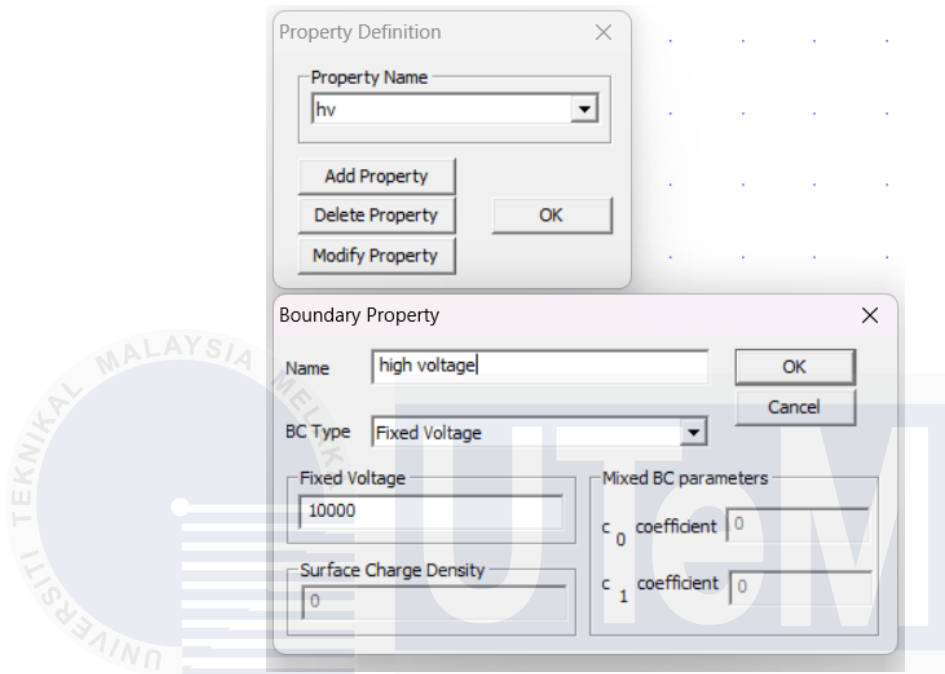


Figure 3.10: Block Property dialog for boundary

To start creating the model, add node tool and enter the X and Y coordinates in the input boxes that appear, such as X = 0 and Y = 1 in Figure 3.11. After placing all of the coordinates, use the tool bar buttons to complete the other components.

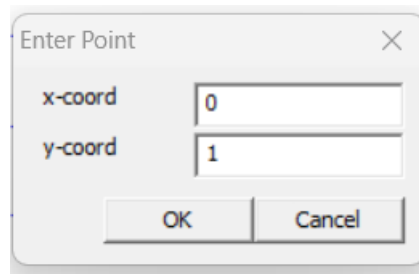


Figure 3.11: Block Property for coordinate point

Figure 3.12 shows the block property the selected block. When labelling the block components, insert mesh size as 0.001. It is set for a high level of detail and accuracy in the simulation results.

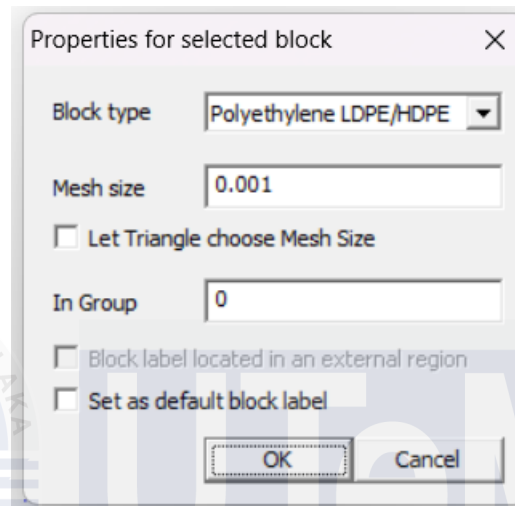


Figure 3.12: Mesh size parameter dialog

Figure 3.13 shows the nanocomposites modelling after inserting all the parameters.

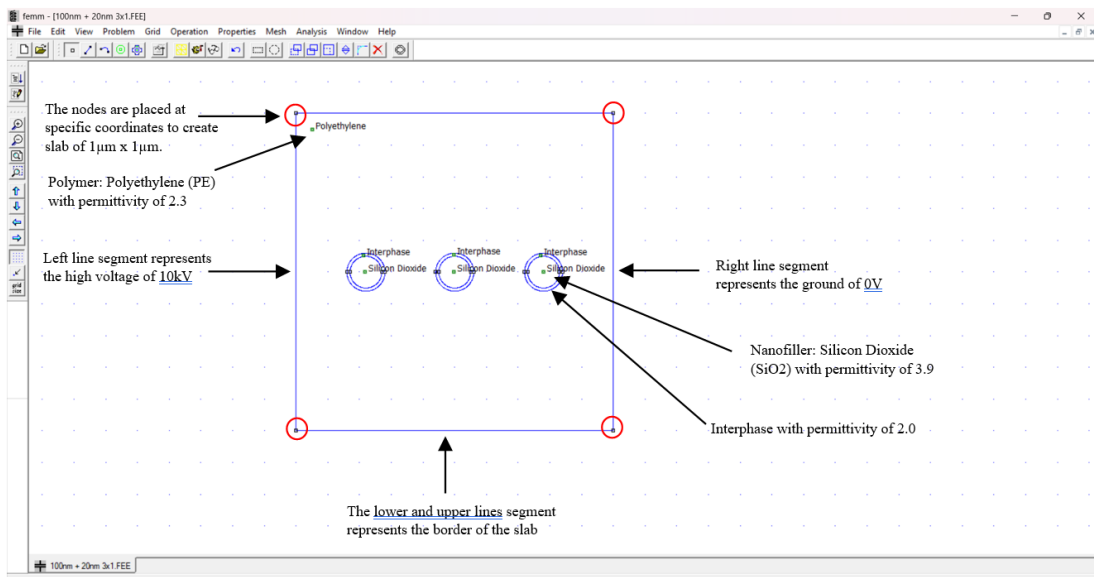


Figure 3.13: Nanocomposites Modelling

Figure 3.14 shows the toolbar buttons for analysis tasks which are meshing and analysing the model and viewing the results. The first button (yellow mesh icon) in Figure 3.12 is the mesh generator. The mesh size determines the resolution of the finite element mesh used in the simulation. The electrostatics post processing is used to view solutions generated by the belasolv solver. The second button, with the “hand-crank” icon, executes the solver, Belasolv.exe. The “big magnifying glass” icon is used to run the postprocessor once the analysis is finished.



Figure 3.14: Toolbar buttons for starting analysis tasks

After running the result, it will appear in voltage (V) display as shown in figure 3.15.

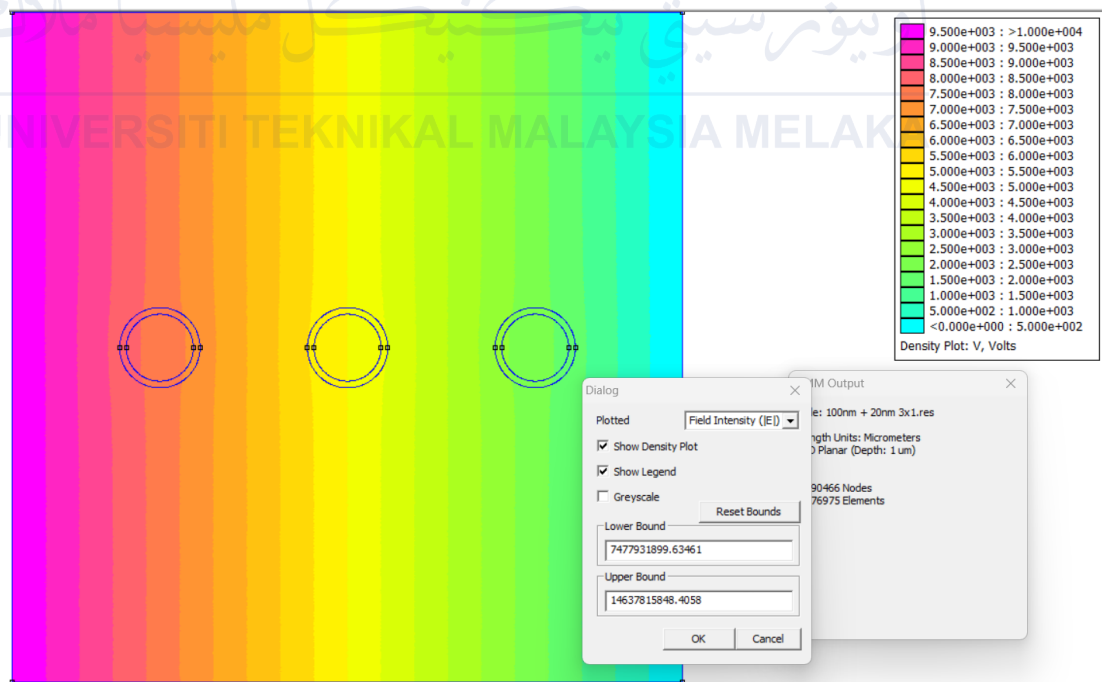


Figure 3.15: Display result in voltage (V)

To change the display from voltage to field intensity ( $|E|$ ) in the results, use the “Contour Plot” button (third button from the left) to bring up the plot options. In the plot options, select to display the field intensity ( $|E|$ ) in Figure 3.16.



Figure 3.16: Buttons that facilitate the analysis of the simulated model

The field intensity will display as show in figure below. Field intensity refers to the strength and direction of the electric at various points in the simulated domain. The unit of field intensity are volts per meter (V/m) for the electric field.



Figure 3.17: Field intensity display (V/m)

## CHAPTER 4

### RESULTS AND DISCUSSIONS

#### 4.1 Introduction

This chapter discusses the simulation result on electric field intensity on polymer nanocomposites using FEMM 4.2 software simulation. The result and analysis of simulation will be discussed to understand the effect electric field intensity with the variation of five nanoparticle sizes. It is expected to achieve the first objective which is able to model the electric field distribution in polymer composites using Finite Elements Method Magnetics (FEMM) 4.2 software.

#### 4.2 Unfilled Polyethylene (PE)

Figure 4.1 below shows the electric field intensity,  $|E|$  in an unfilled PE. The electric field was found to be homogeneously distributed in the unfilled polymer at the lowest range of intensity. There are no electric field distributed around the unfilled PE, thus the value of the intensity,  $|E| = 0$ .

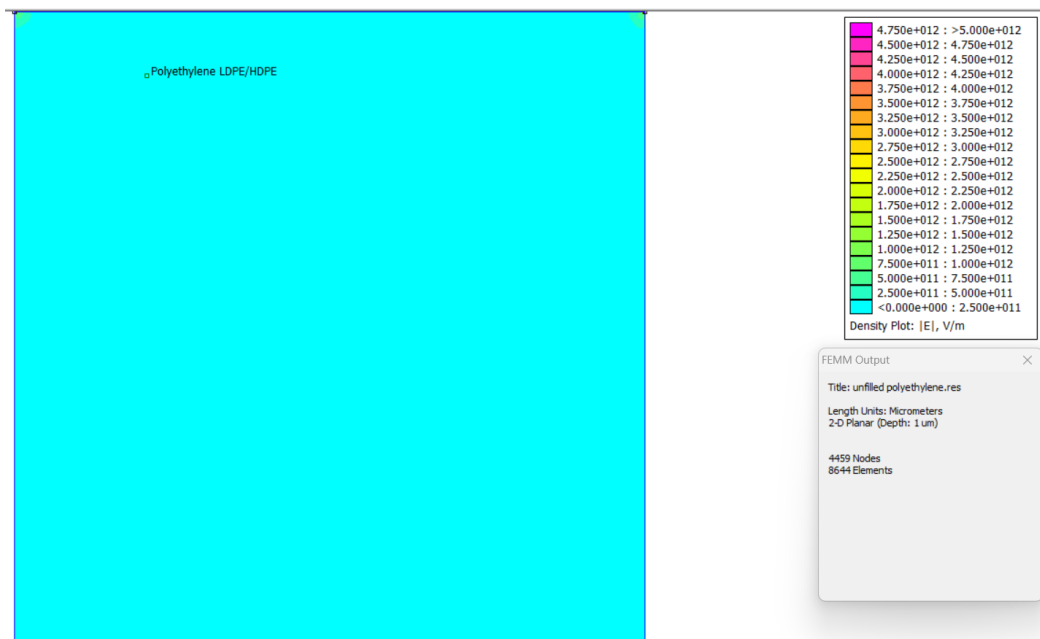


Figure 4.1: Intensity Color Contour of Unfilled PE

From this result in Figure 4.2, it can be summarized that there was no electric field intensity observed from there was no contour color generated due no nanofiller has been added.

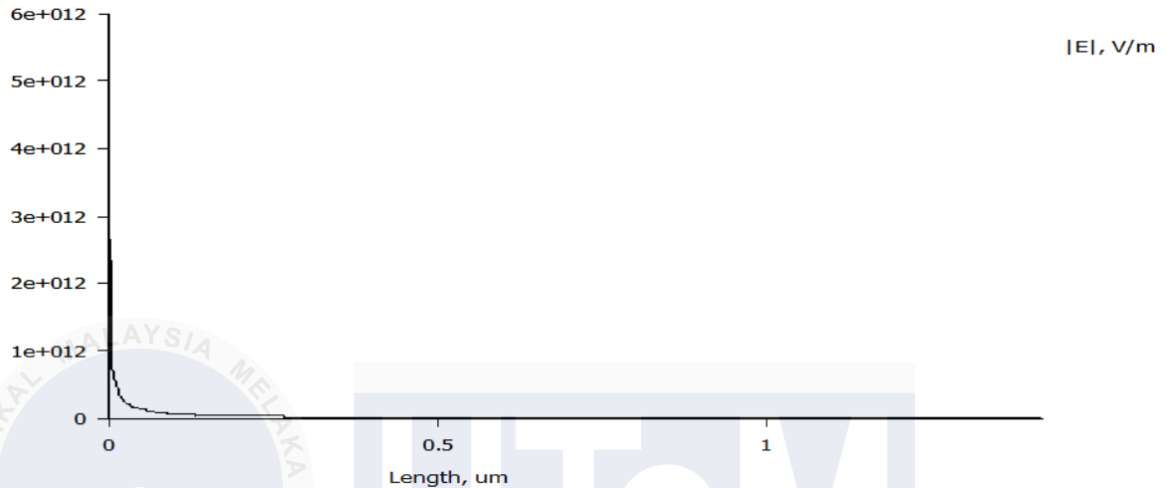


Figure 4.2: Graph

### 4.3 Polyethylene Nanocomposites at Different Filler Size at 10nm Interphase

This section discusses the performance of electric field intensity of the polymer nanocomposites. It provides on the effects of electric field distribution on the results of PE Nanocomposites at different filler sizes. For this, section, there are five sizes of nanoparticles were simulated, which 20nm, 40nm, 60nm, 80nm and 100nm at interphase of 10nm and 20nm.

#### 4.3.1 PE at 20nm nanoparticle with 10nm interphase

The first sample is the PE at 20nm nanoparticle with 10nm interphase. Figure 4.3 shows (a) electric field distribution and (b) close-up  $\text{SiO}_2$  nanomaterial with 10nm interphase.

Based on Figure 4.3 (a), it is shown that the peak intensity is at  $1.396 \times 10^{10}$  V/m. The curve graph is represented as a filler size of a nanoparticle. It shows that there is a slight curve due to nanoparticle existence. When the nanomaterial is being close-up, it can be seen clearer the regions of concentrated field intensity around the nanomaterial in Figure 3.4 (b). The color gradient of the field intensity regions in is in green and yellow low-intensity. The intensity shows it is around  $1.047 \times 10^{10}$  V/m to  $1.082 \times 10^{10}$  V/m.

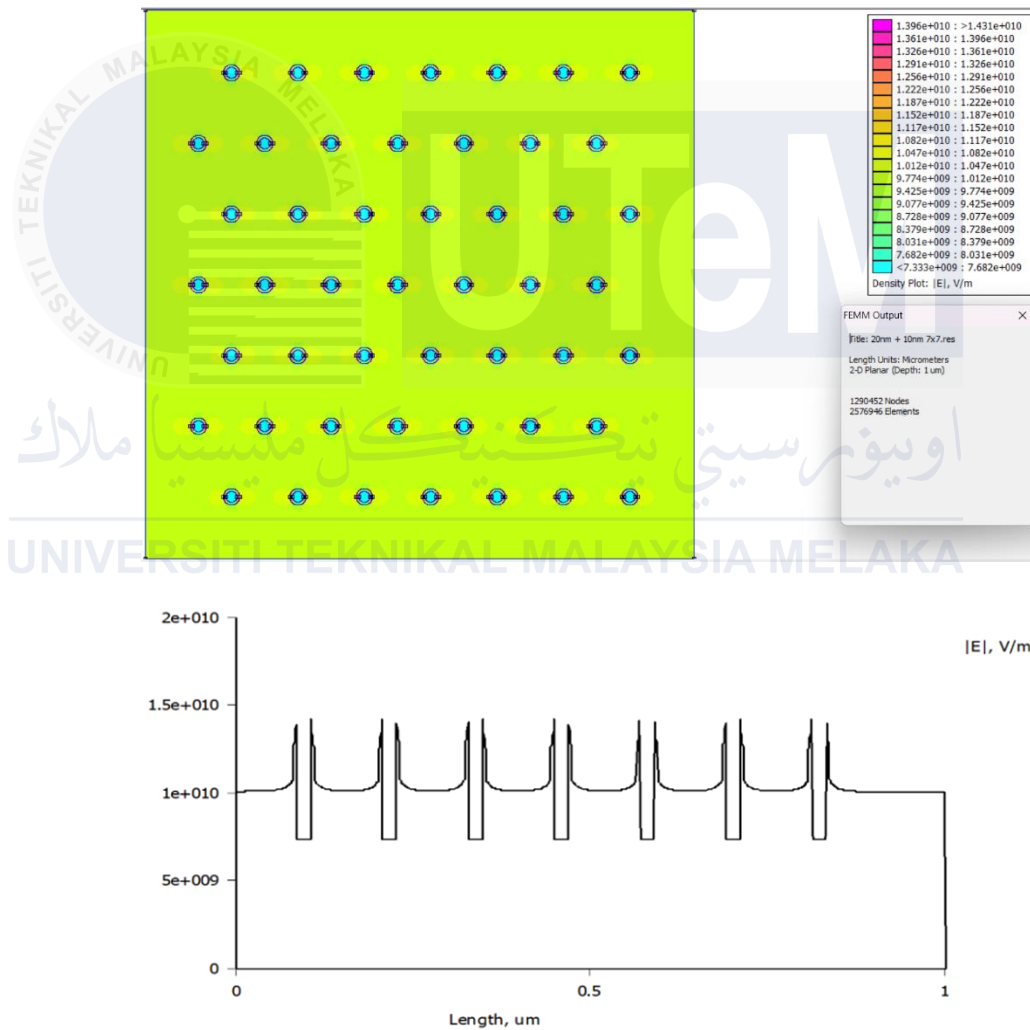


Figure 4.3 (a)

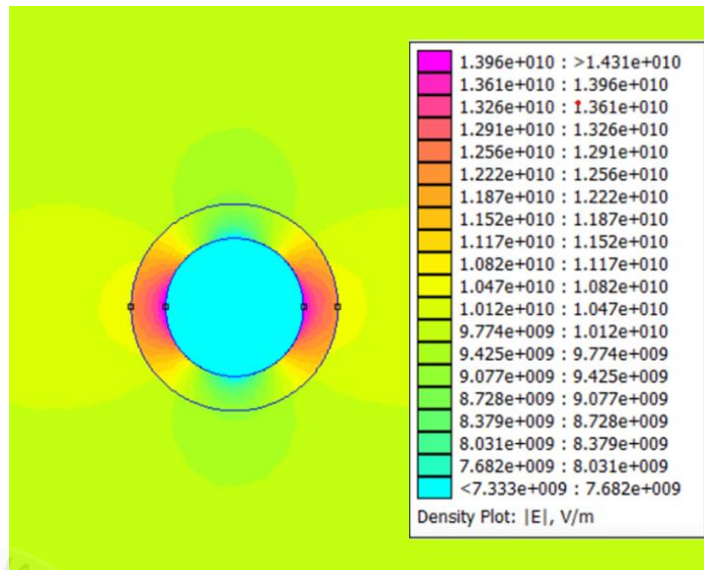
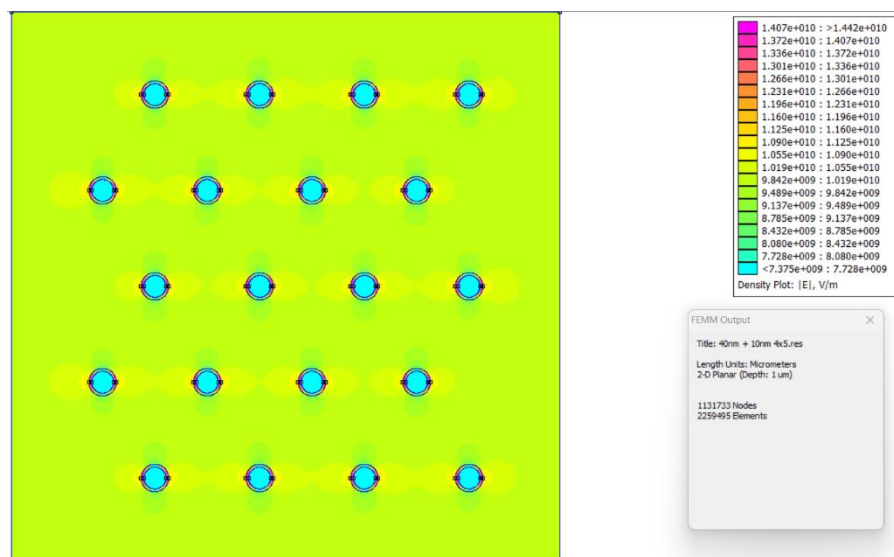


Figure 4.3 (b)

#### 4.3.2 PE at 40nm nanoparticle with 10nm interphase

Sample 2 is PE at 40nm nanoparticle with 10nm interphase. Based on Figure 4.4 (a), it is shown that the peak intensity is at  $1.407 \times 10^{10}$  V/m. While the curve in the graph getting bigger as the size of nanoparticles starting to increase. There are slightly increase of  $1.1 \times 10^{10}$  intensity compared to sample 1. The color gradient of the intensity regions in Figure 4.4 (b) is in green and yellow low-intensity, but the green region is getting wider than in sample 1. The intensity shows it is around  $1.125 \times 10^{10}$  V/m to  $1.160 \times 10^{10}$  V/m.





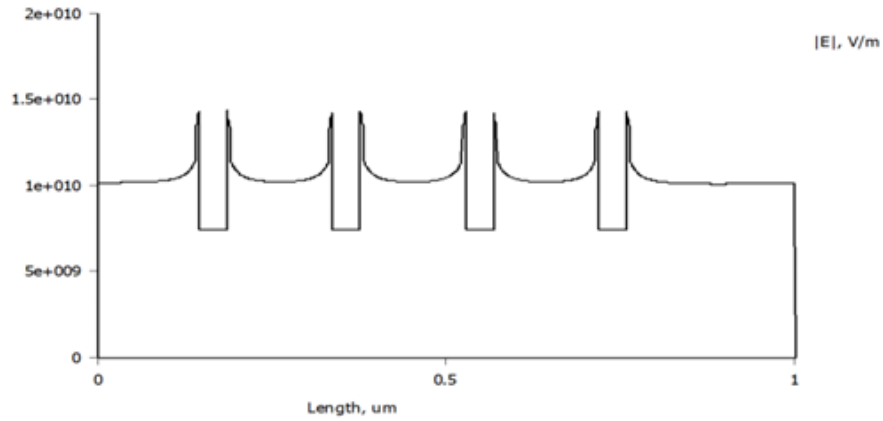


Figure 4.4 (a)

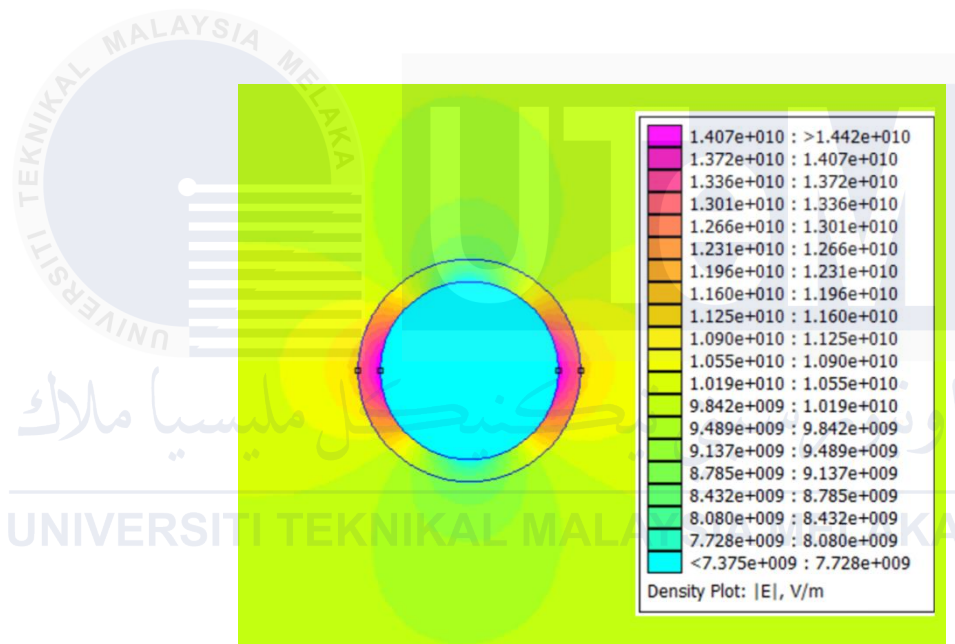


Figure 4.4 (b)

### 4.3.3 PE at 60nm nanoparticle with 10nm interphase

Sample 3 is the PE at 60nm nanoparticle with 10nm interphase. Based on Figure 4.5 (a), It is shown that the peak intensity is at  $1.414 \times 10^{10}$  V/m. The intensity increases as the size of nanomaterial increases. While the curve in the graph getting bigger as the size of nanoparticles starting to increase. The color gradient of the intensity regions in Figure 4.5 (b) starting to develop more layers of green and yellow intensity. The intensity shows it is around  $1.130 \times 10^{10}$  V/m to  $1.166 \times 10^{10}$  V/m.

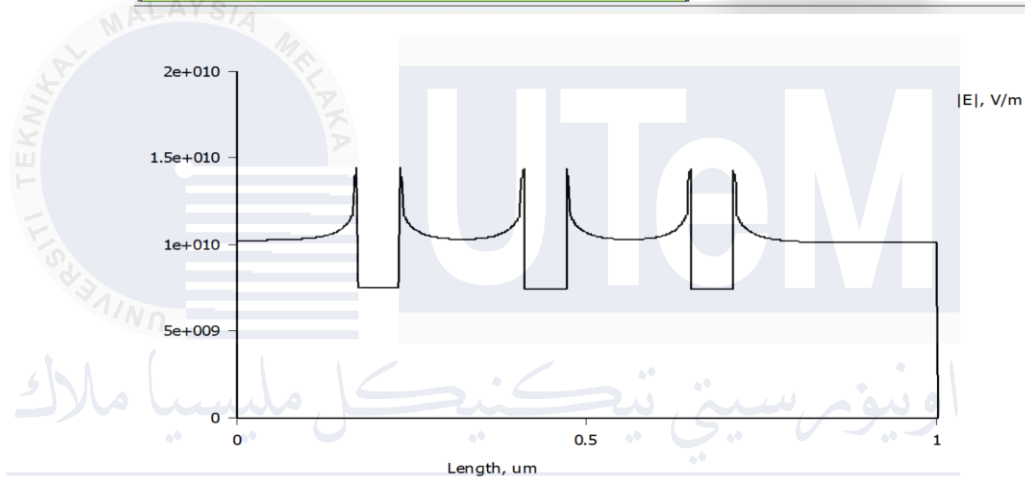
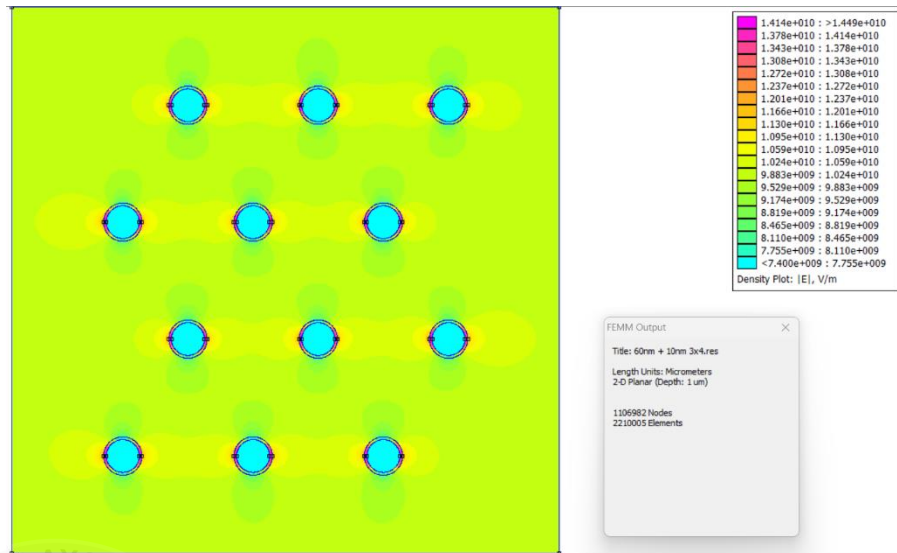


Figure 4.5 (a)

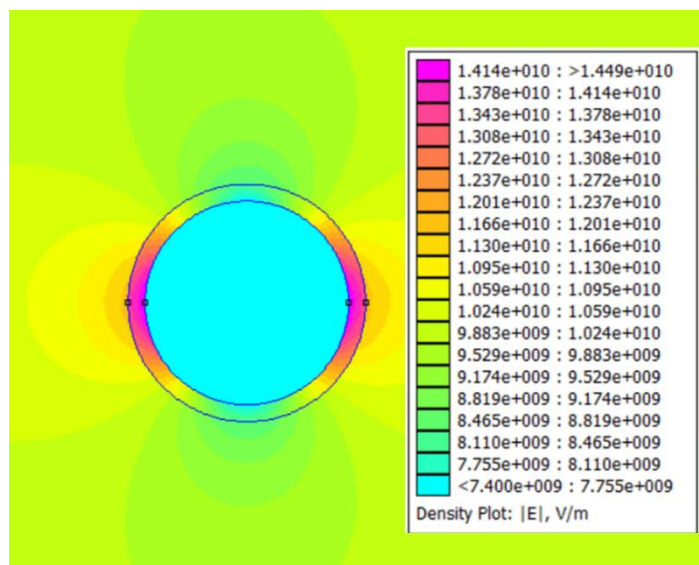


Figure 4.5 (b)

#### 4.3.4 PE at 80nm nanoparticle with 10nm interphase

Sample 4 is the PE at 80nm nanoparticle with 10nm interphase. Based on Figure 4.6 (a), It is shown that the peak intensity is at  $1.415 \times 10^{10}$  V/m. The intensity increases by very small amount from  $1.414 \times 10^{10}$  V/m to  $1.415 \times 10^{10}$  V/m. While the curve in the graph getting bigger as the size of nanoparticles starting to increase. The color gradient of the intensity regions in Figure 4.6 (b) starting to generate more layers of green and yellow intensity and starting to spread wider. The intensity shows it is around  $1.166 \times 10^{10}$  V/m to  $1.202 \times 10^{10}$  V/m.

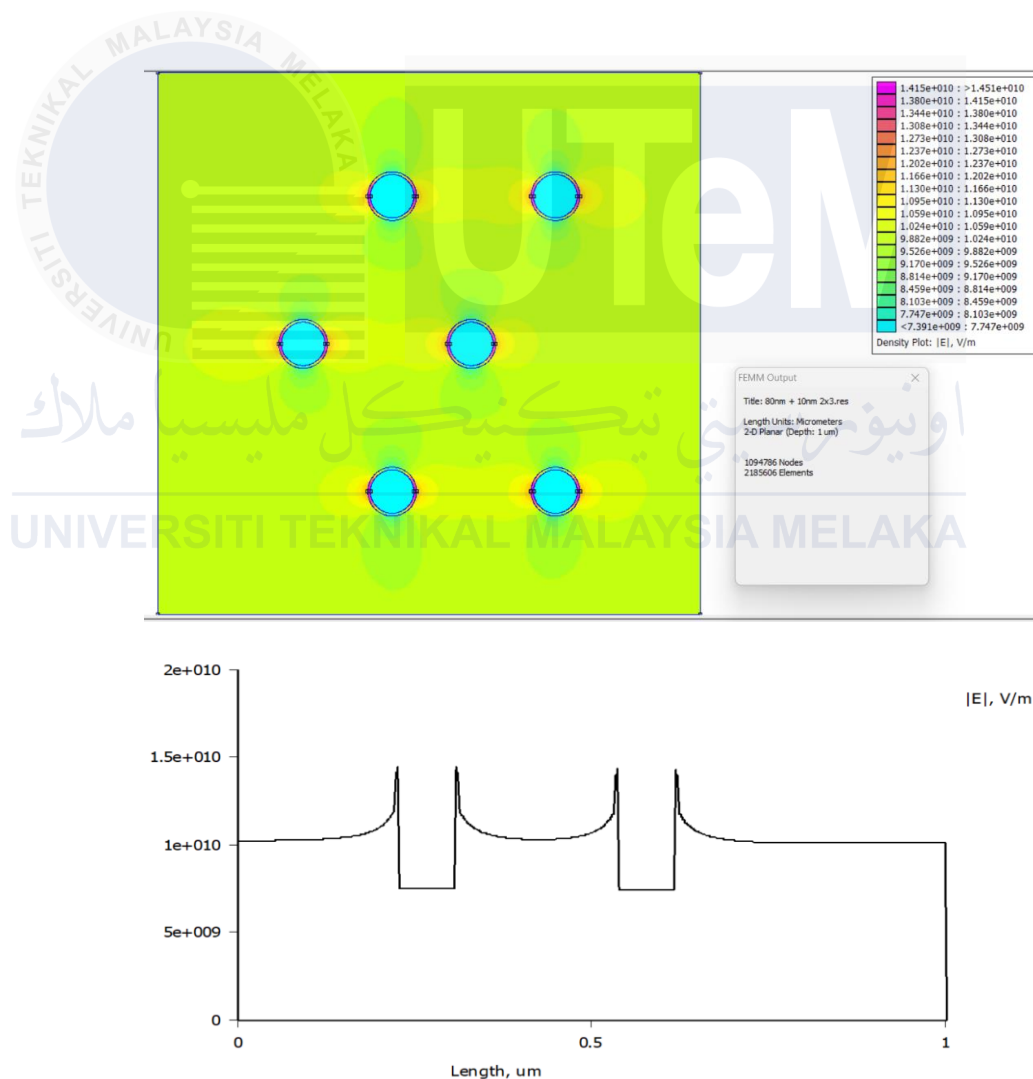


Figure 4.6 (a)

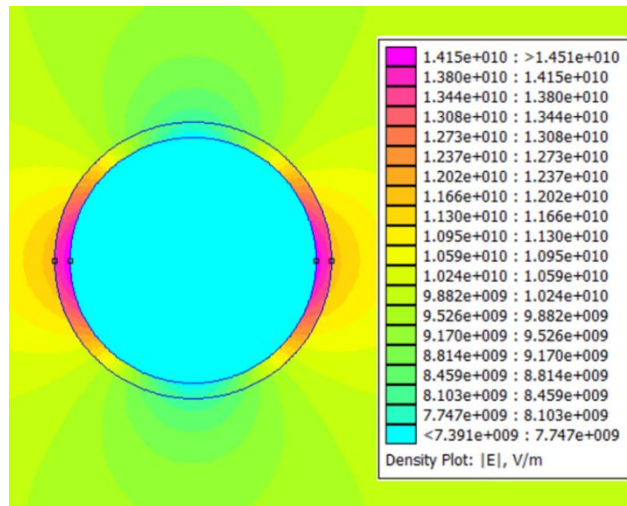


Figure 4.6 (b)

#### 4.3.5 PE at 100nm nanoparticle with 10nm interphase

Sample 5 is the PE at 100nm nanoparticle with 10nm interphase. Based on Figure 4.7 (a), It is shown that the peak intensity is at  $1.419 \times 10^{10}$  V/m. The intensity of this sample is the highest among other nanoparticles size of 10nm interphase. While the curve in the graph is the biggest compared to other sizes. The color gradient of the intensity regions in Figure 4.7 (b) starting to generate more layers and brighter color of green and yellow intensity, spreading wider and touch other region of other nanomaterial around. The intensity shows it is around  $1.170 \times 10^{10}$  V/m to  $1.206 \times 10^{10}$  V/m.

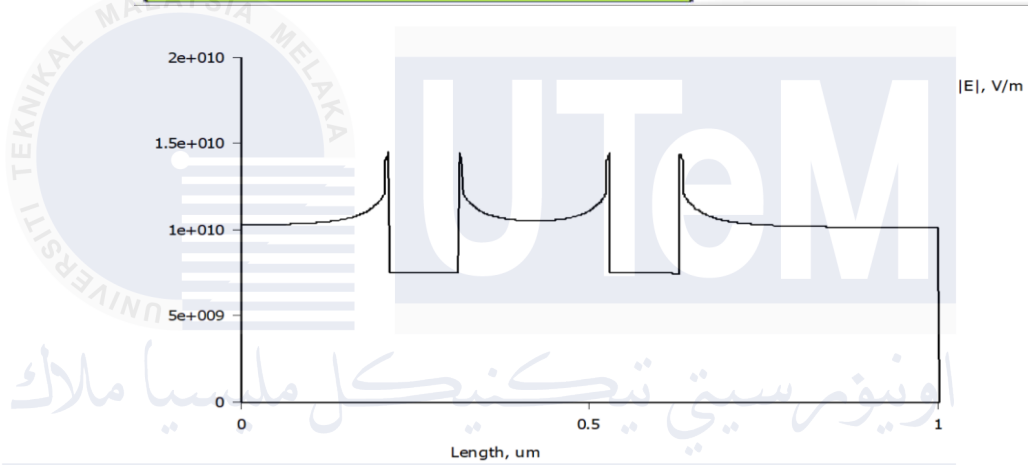
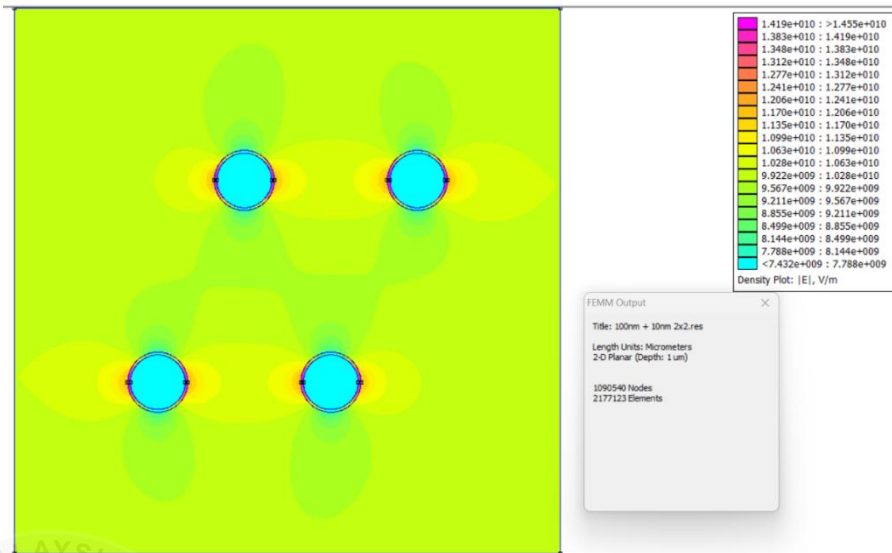


Figure 4.7 (a)

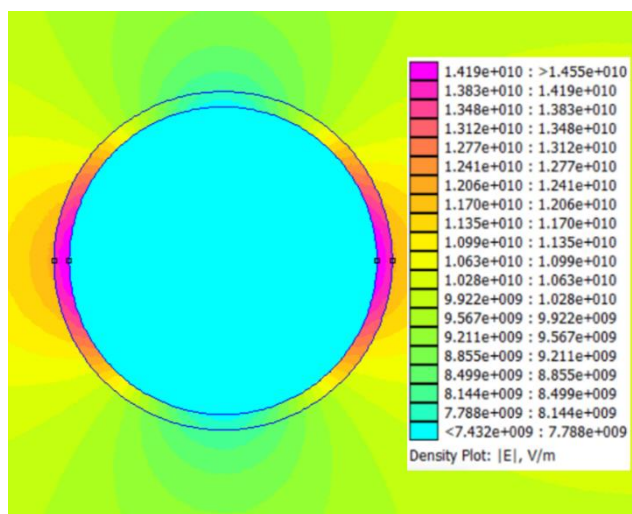


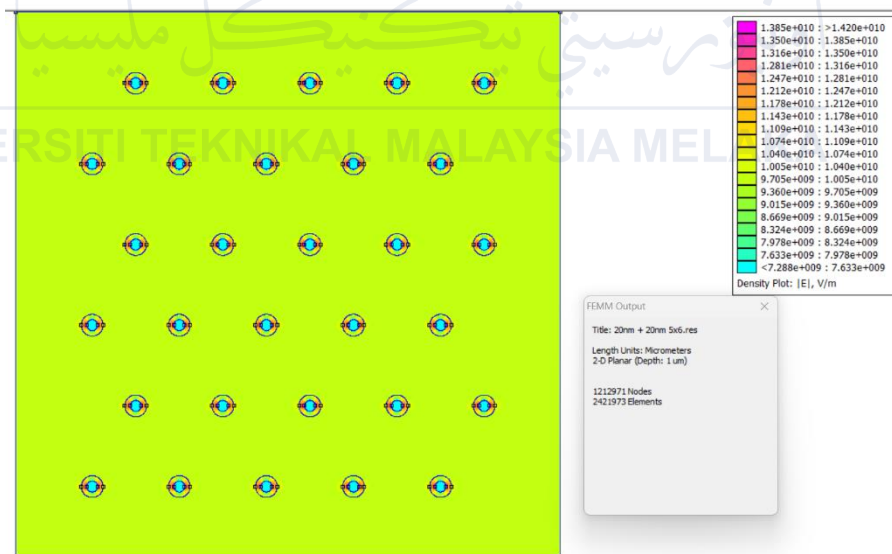
Figure 4.7 (b)

## 4.4 Polyethylene Nanocomposites at Different Filler Size at 20nm Interphase

### 4.4.1 PE at 20nm nanoparticle with 20nm interphase

The first sample is the PE at 20nm nanoparticle with 20nm interphase. Figure 4.3 shows (a) electric field distribution and (b) close-up SiO<sub>2</sub> nanomaterial with 10nm interphase.

Based on Figure 4.8 (a), It is shown that the peak intensity is at  $1.385 \times 10^{10}$  V/m. The curve graph is represented as a filler size of a nanoparticle. It shows that there is a slight curve due to nanoparticle existence. When the nanomaterial is being close-up, it can be seen clearer the regions of concentrated field intensity around the nanomaterial in Figure 4.8 (b). The color gradient of the field intensity regions is in yellow low intensity. The intensity shows it is around  $1.005 \times 10^{10}$  V/m to  $1.040 \times 10^{10}$  V/m.



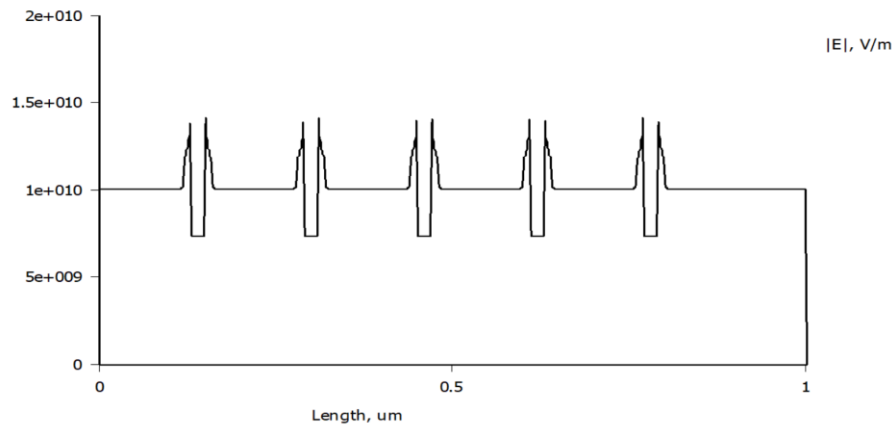


Figure 4.8 (a)

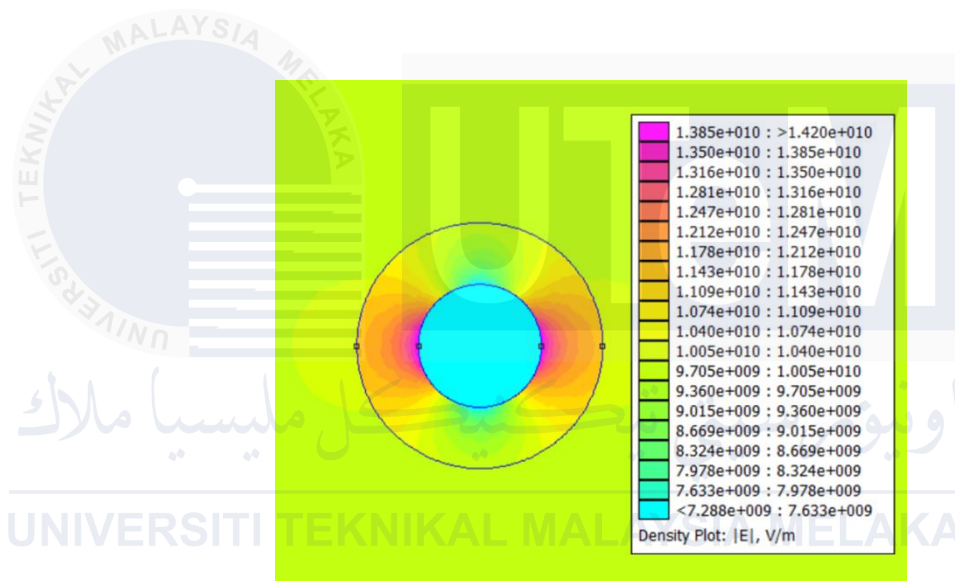


Figure 4.8 (b)

#### 4.4.2 PE at 40nm nanoparticle with 20nm interphase

Sample 2 is the PE at 40nm nanoparticle with 20nm interphase. Based on Figure 4.9 (a), It is shown that the peak intensity is at  $1.394 \times 10^{10}$  V/m. There are slightly increase of  $9 \times 10^7$  intensity compared to sample 1. While the curve in the graph getting bigger as the size of nanoparticles starting to increase. The color gradient of the intensity regions in Figure 4.9 (b) is in green and yellow low-intensity, the green intensity starting to appear. The intensity shows it is around  $1.046 \times 10^{10}$  V/m to  $1.081 \times 10^{10}$  V/m.

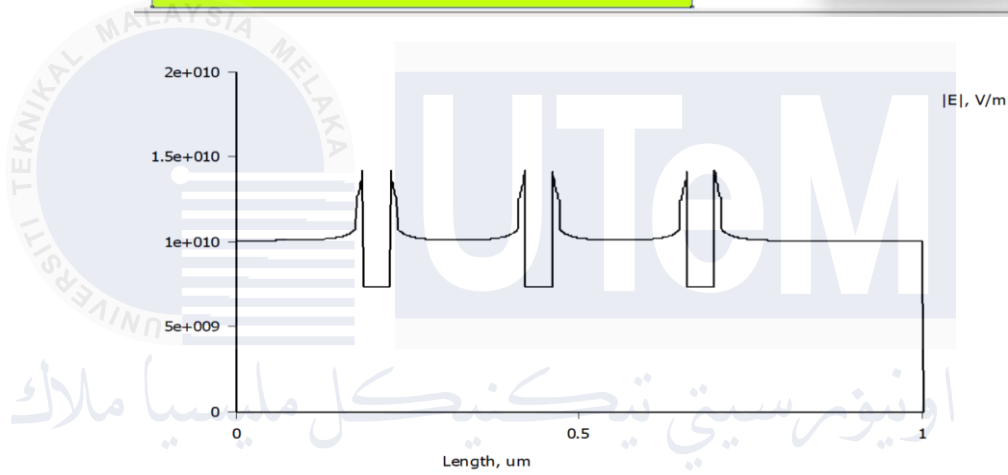
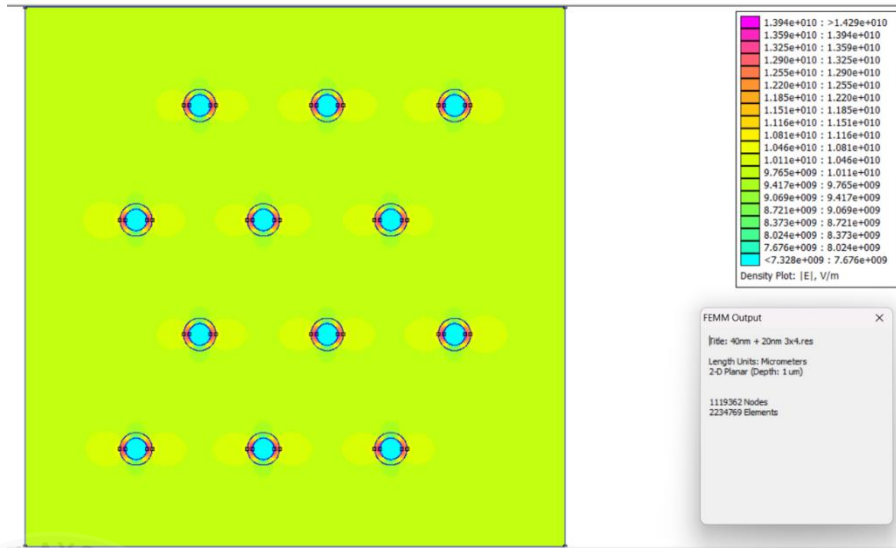


Figure 4.9 (a)

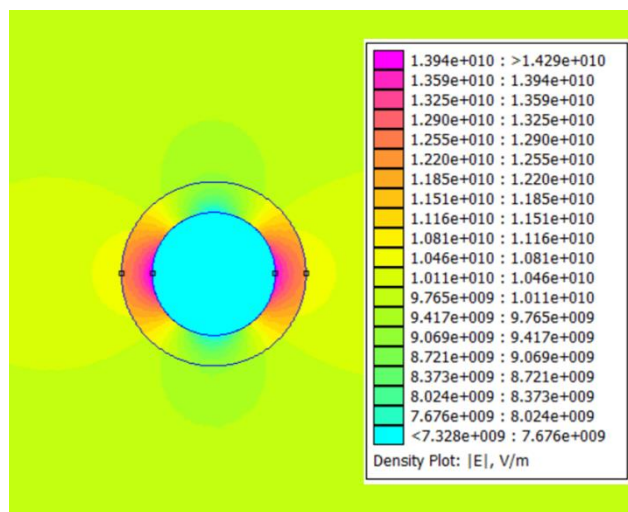


Figure 4.9 (b)



#### 4.4.3 PE at 60nm nanoparticle with 20nm interphase

Sample 3 is the PE at 60nm nanoparticle with 20nm interphase. Based on Figure 4.10 (a), It is shown that the peak intensity is at  $1.4 \times 10^{10}$  V/m. The intensity increases as the size of nanomaterial increases. While the curve in the graph getting bigger as the size of nanoparticles starting to increase. The color gradient of the intensity regions in Figure 4.10 (b) is in green and yellow intensity, and it is starting to spread around it. The intensity shows it is around  $1.085 \times 10^{10}$  V/m to  $1.120 \times 10^{10}$  V/m.

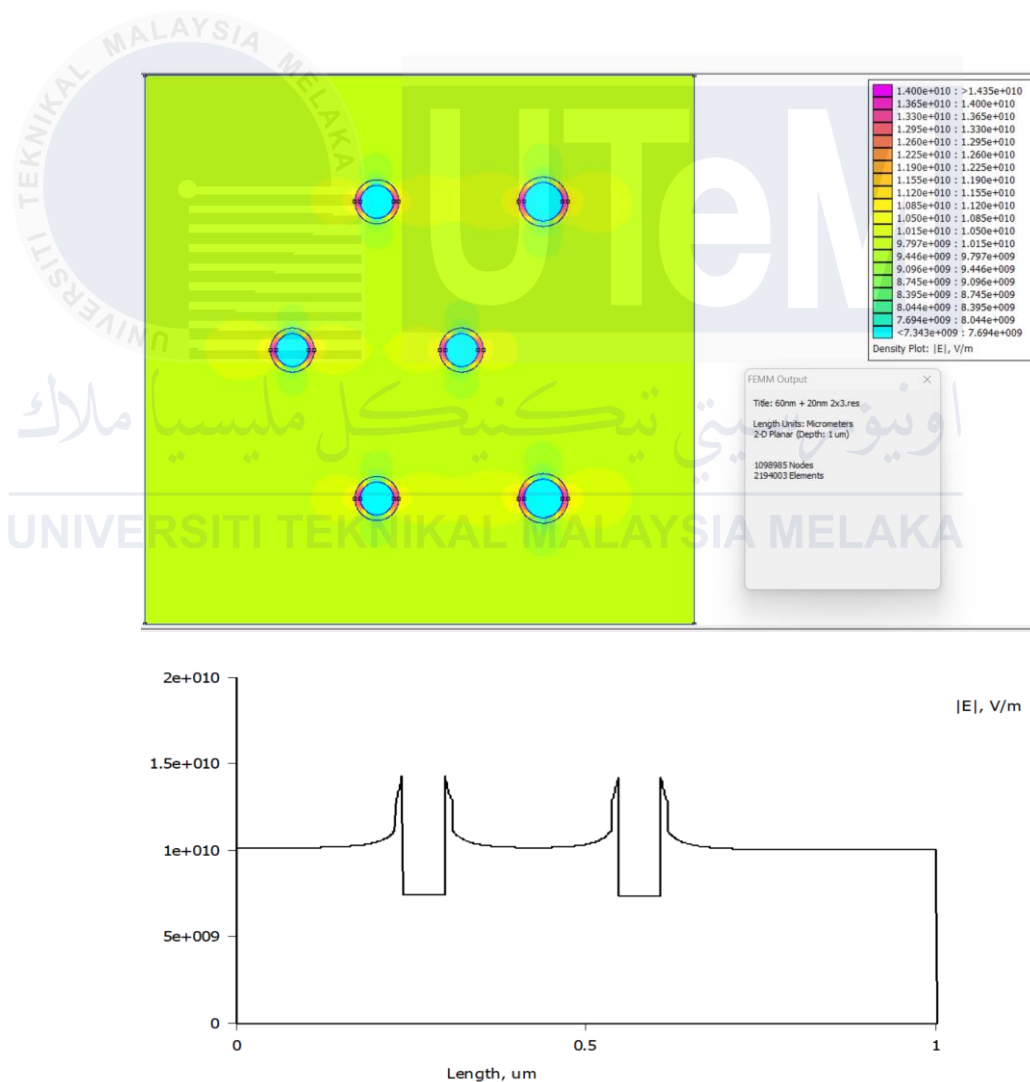


Figure 4.10 (a)

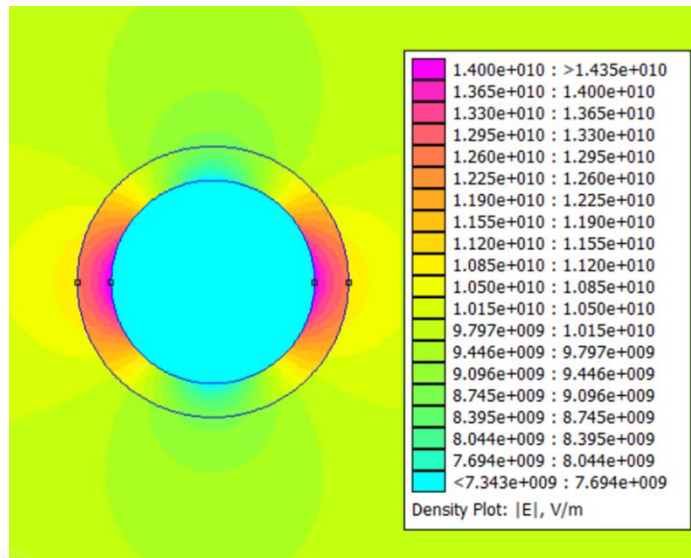
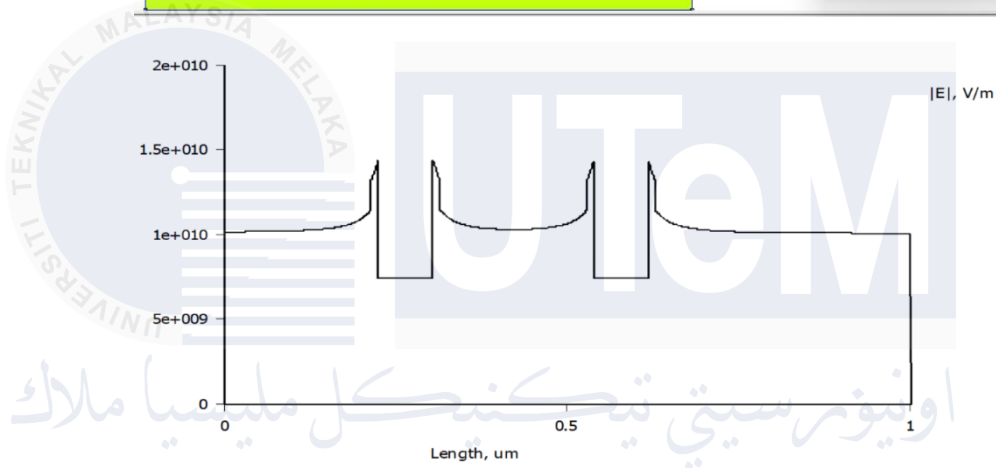
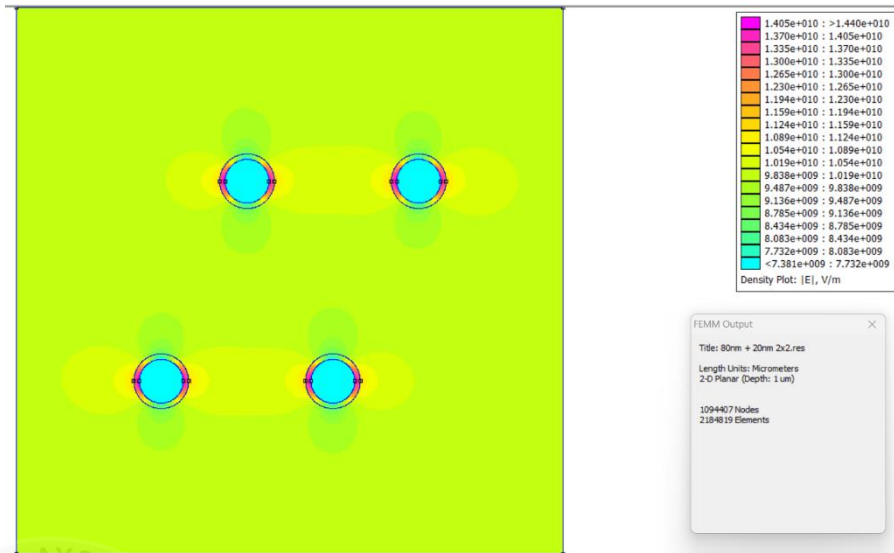


Figure 4.10 (b)

#### 4.4.4 PE at 80nm nanoparticle with 20nm interphase

Sample 4 is the PE at 80nm nanoparticle with 20nm interphase. Based on Figure 4.11 (a), It is shown that the peak intensity is at  $1.455 \times 10^{10}$  V/m. The intensity increases by very small amount from  $1.4 \times 10^{10}$  V/m to  $1.405 \times 10^{10}$  V/m. While the curve in the graph getting bigger as the size of nanoparticles starting to increase. The color gradient of the intensity regions in Figure 4.11 (b) starting to generate more layers of green and yellow intensity and spread wider. The intensity shows it is around  $1.124 \times 10^{10}$  V/m to  $1.159 \times 10^{10}$  V/m.



UNIVERSITI TEKNIKAL MALAYSIA MELAKA Figure 4.11 (a)

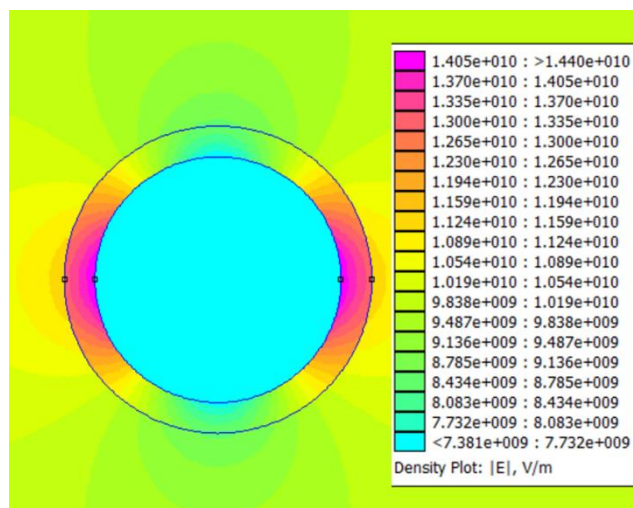


Figure 4.11 (b)

#### 4.4.5 PE at 100nm nanoparticle with 20nm interphase

Sample 5 is the PE at 100nm nanoparticle with 10nm interphase. Based on Figure 4.12 (a), It is shown that the peak intensity is at  $1.428 \times 10^{10}$  V/m. The intensity of this sample is the highest among other nanoparticles size of 20nm interphase. While the curve in the graph is the biggest compared to other sizes. The color gradient of the intensity regions in Figure 4.12 (b) starting to generate more layers and brighter color of green and yellow intensity, spreading wider and touch other region of other nanomaterial around. The intensity shows it is around  $1.142 \times 10^{10}$  V/m to  $1.177 \times 10^{10}$  V/m.

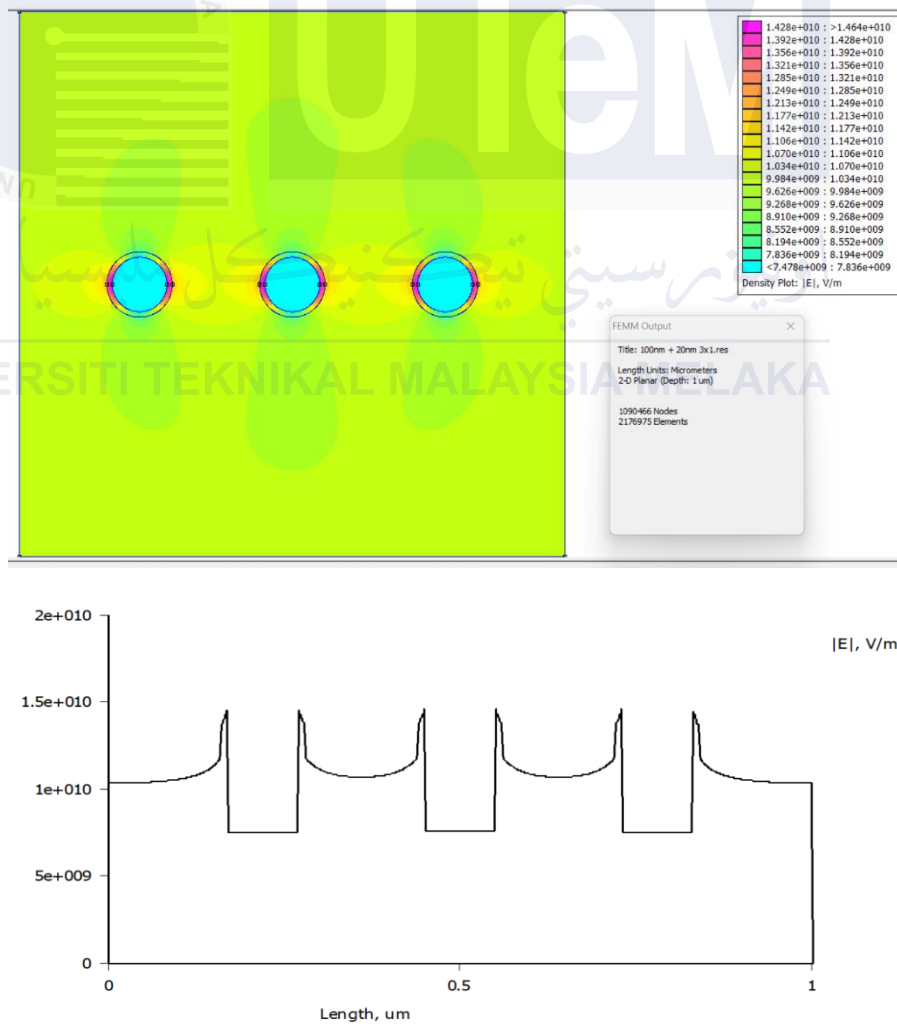


Figure 4.12 (a)

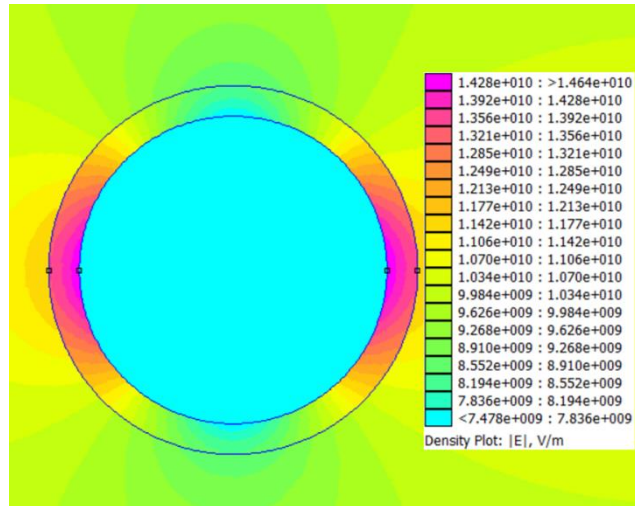


Figure 4.12(b)

Based on the results in Table 4.1, as the nanoparticle size increases, there is a slight trend of the electric field distribution increasing. This indicates that larger nanoparticles may have a more pronounced effect on the electric field distribution within the nanocomposite. The electric field distribution can also be influenced by the interphase thickness. The data shows that thicker interphase (20nm) results in a lower electric field intensity compared to a thinner interphase (10nm) for the same nanoparticle size.

Table 4.1: Summary of the results

Nanoparticle Size	Electric Field Distribution	
	Interphase 10nm	Interphase 20nm
20nm	1.396 x 10 <sup>10</sup> V/m – 1.431 x 10 <sup>10</sup> V/m	1.385 x 10 <sup>10</sup> V/m – 1.420 x 10 <sup>10</sup> V/m
40nm	1.407 x 10 <sup>10</sup> V/m – 1.442 x 10 <sup>10</sup> V/m	1.394 x 10 <sup>10</sup> V/m – 1.429 x 10 <sup>10</sup> V/m
60nm	1.414 x 10 <sup>10</sup> V/m – 1.449 x 10 <sup>10</sup> V/m	1.40 x 10 <sup>10</sup> V/m – 1.435 x 10 <sup>10</sup> V/m
80nm	1.415 x 10 <sup>10</sup> V/m – 1.451 x 10 <sup>10</sup> V/m	1.405 x 10 <sup>10</sup> V/m – 1.440 x 10 <sup>10</sup> V/m
100nm	1.419 x 10 <sup>10</sup> V/m – 1.455 x 10 <sup>10</sup> V/m	1.428 x 10 <sup>10</sup> V/m – 1.464 x 10 <sup>10</sup> V/m

Based on Figure 4.13, generally, as the size of nanoparticle increases, the range of field intensity also tends to increase. This indicates that larger nanoparticles have a more significant impact on the electric field distribution within the nanocomposite compared to smaller nanoparticles. It can be seen in the table above that when the size of nanoparticle increases, the field intensity increases. This trend is same for both 10nm and 20nm of interphase. This research purpose is achieved when we compared to previous research studies.

There is a trend of increasing electric field intensity with increasing nanoparticle size, regardless of the interphase thickness. However, this trend is disrupted for the 20nm interphase thickness, where the electric field intensity for nanoparticle sizes 20nm to 80nm is lower compared to the 10nm interphase thickness. The data suggests that the relationship between nanoparticle size and electric field intensity is influenced by the interphase thickness. While larger nanoparticles generally lead to higher electric field intensities, this trend is altered by the presence of a 20nm interphase, resulting in lower intensities for nanoparticle sizes 20nm to 80nm.

The sudden increase in electric field intensity for the 100nm nanoparticle size with a thicker interphase of 20nm compared to 10nm could be attributed to the change in the interparticle distance and the resulting interactions between nanoparticles. In the 20nm interphase, the nanoparticles may be closer together, leading to a more concentrated electric field distribution and thus higher intensity values. Conversely, in the 10nm interphase, the nanoparticles may be more dispersed, resulting in a less concentrated electric field distribution and lower intensity values.

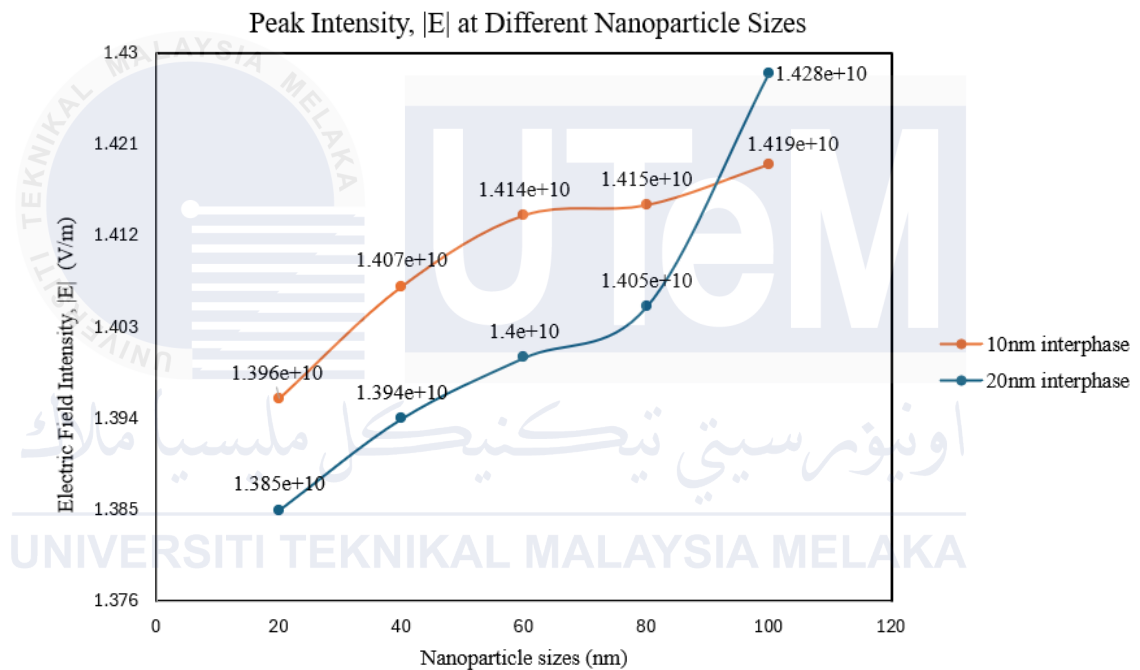


Figure 13: Comparison of different nanoparticle sizes at interphase of 10nm and 20nm

## CHAPTER 5

### CONCLUSION AND RECOMMENDATIONS

#### 5.1 Conclusion

This study investigated the effect of electric field distribution in polymer nanocomposites under varying filler sizes using FEMM 4.2 software. Five nanoparticle sizes ranging from 20nm, 40nm, 60nm, 80nm, and 100nm were modeled in a polyethylene polymer matrix. The simulation results showed that the electric field intensity increases with larger nanoparticle sizes. This is likely due to the nanoparticles providing more surface area for electric field lines to concentrate as the size increases. Additionally, the effect of interphase thicknesses of 10nm and 20nm was analyzed. The simulation results showed that the electric field intensity increases with larger nanoparticle sizes, likely due to increased surface area for electric field concentration. Moreover, it was observed that a thinner interphase (10nm) results in higher electric field intensities compared to a thicker interphase (20nm), however noticeable in larger nanoparticles (100nm) in thicker interphase (20nm). These insights underscore the importance of both nanoparticle size and interphase thickness in optimizing the electric field characteristics within nanocomposites. The objective to model the electric field distribution in polymer composites and determine the effect of different filler sizes using FEMM was achieved. The modeling approach and simulations provided insights into how nanoparticle sizing influences the electric field characteristics with the inclusion of interphase within the nanocomposite material. This has implications for designing insulation materials with optimized electric field performance.

#### 5.2 Future Work

For future work, it is recommended to broaden the investigation by exploring the impact of various nanofillers on the electric field distribution within polymer nanocomposites and comparing their performance in terms of conductivity, strength, and thermal stability. Additionally, extending the study to examine the influence of filler concentration, analyzing the effect of temperature variations on electric field distribution, and conducting dynamic simulations to observe the material's behavior



under changing electrical conditions would provide a more comprehensive understanding. Experimental validation is crucial to confirm simulation results, and a detailed exploration of the interphase region between filler and matrix is demanded. Implementing multiscale modeling techniques, assessing environmental impacts, and applying optimization algorithms to find the optimal combination of filler size and concentration can further contribute to the development of enhanced insulating materials. Lastly, applying the study's findings to specific electrical components or systems and evaluating practical implications in real-world applications would be valuable for advancing the field.



## REFERENCES

- [1] J. Huang, J. Zhou, and M. Liu, "Interphase in Polymer Nanocomposites," *JACS Au*, vol. 2, no. 2. pp. 280–291, Feb. 28, 2022. doi: 10.1021/jacsau.1c00430.
- [2] M. Okamoto, "Polymer Nanocomposites," *Eng*, vol. 4, no. 1. Multidisciplinary Digital Publishing Institute (MDPI), pp. 457–479, Mar. 01, 2023. doi: 10.3390/eng4010028.
- [3] K. Yiew Lau and M. M. Afendi Piah, "Polymer Nanocomposites in High Voltage Electrical Insulation Perspective: A Review." [Online]. Available: <https://www.researchgate.net/publication/264880479>
- [4] IEEE Power & Energy Society, Fla. IEEE PES Transmission and Distribution Conference and Exposition 2012.05.07-10 Orlando, and Fla. T & D 2012.05.07-10 Orlando, *IEEE PES Transmission and Distribution Conference and Exposition (T & D), 2012 7-10 May 2012, Orlando, FL, USA.*
- [5] M. I. B. Tavares, E. O. da Silva, P. R. C. da Silva, and L. R. de Menezes, "Polymer Nanocomposites," in *Nanostructured Materials*, M. S. Seehra, Ed., Rijeka: IntechOpen, 2017. doi: 10.5772/intechopen.68142.
- [6] T. Tanaka, M. Kozako, N. Fuse, and Y. Ohki, "Proposal of a Multi-core Model for Polymer Nanocomposite Dielectrics," 2005.
- [7] D.Lopez, "High-voltage insulators: characteristics, types and use," Publisher.
- [8] Admin, "Importance of High Voltage Insulators in power lines?," Publisher.
- [9] M. Yousaf *et al.*, "Microstructural and mechanical characterization of high strength porcelain insulators for power transmission and distribution applications," *Ceram Int*, vol. 48, no. 2, pp. 1603–1610, Jan. 2022, doi: 10.1016/J.CERAMINT.2021.09.239.

- [10] Prashant Digital, "Types of Insulators Used in Power Transmission Lines," Publisher.
- [11] Sharip, M., & Ridhuan, M. (2015). Electric field distribution in nanocomposites containing one-dimensional nanofiller. <http://eprints.utm.my/id/eprint/53888/>
- [12] K. Y. Lau *et al.*, "Modeling of polymer nanocomposites: Permittivity vs. electric field intensity," in *Conference Proceeding - 2014 IEEE International Conference on Power and Energy, PECon 2014*, Institute of Electrical and Electronics Engineers Inc., Mar. 2014, pp. 140–145. doi: 10.1109/PECON.2014.7062429.
- [13] M. F. Fréchette, M. Trudeau, H. D. Alamdari, and S. Boily, "Introductory remarks on nanoDielectrics," *Conference on Electrical Insulation and Dielectric Phenomena (CEIDP), Annual Report*, pp. 92–99, 2001, doi: 10.1109/CEIDP.2001.963496.
- [14] I. A. Tsekmes, R. Kochetov, P. H. F. Morshuis, and J. J. Smit, "A unified model for the permittivity and thermal conductivity of epoxy based composites," *J Phys D Appl Phys*, vol. 47, no. 41, Oct. 2014, doi: 10.1088/0022-3727/47/41/415502.
- [15] J. K. Nelson, "Dielectric polymer nanocomposites," *Dielectric Polymer Nanocomposites*, pp. 1–368, 2010, doi: 10.1007/978-1-4419-1591-7/COVER.
- [16] T. Imai, Y. Hirano, H. Hirai, S. Kojima, and T. Shimizu, "Preparation and properties of epoxy-organically modified layered silicate nanocomposites," *Conference Record of IEEE International Symposium on Electrical Insulation*, pp. 379–383, 2002, doi: 10.1109/ELINSL.2002.995955.
- [17] S. Raetzke and J. Kindersberger, "Role of interphase on the resistance to high-voltage arcing, on tracking and erosion of silicone/SiO<sub>2</sub> nanocomposites,"

*IEEE Transactions on Dielectrics and Electrical Insulation*, vol. 17, no. 2, pp. 607–614, Apr. 2010, doi: 10.1109/TDEI.2010.5448118.

- [18] David Meeker, “Finite Element Method Magnetics:Finite Element Method Magnetics.” Aug. 25, 2013.
- [19] M. Ueda, M. Honda, M. Hosokawa, K. Takahashi, and K. Naito, “Performance of Contaminated Bushing of UHV Transmission Systems,” *IEEE Power Engineering Review*, vol. PER-5, no. 4, pp. 45–46, 1985, doi: 10.1109/MPER.1985.5528825.
- [20] M. Tanahashi, “Development of Fabrication Methods of Filler/Polymer Nanocomposites: With Focus on Simple Melt-Compounding-Based Approach without Surface Modification of Nanofillers,” *Materials*, vol. 3, no. 3, p. 1593, 2010, doi: 10.3390/MA3031593.
- [21] “(PDF) Polymer nanocomposites – synthesis techniques, classification and properties.” Accessed: Jun. 09, 2024. [Online]. Available: [https://www.researchgate.net/publication/312327959\\_Polymer\\_nanocomposites\\_-\\_synthesis\\_techniques\\_classification\\_and\\_properties](https://www.researchgate.net/publication/312327959_Polymer_nanocomposites_-_synthesis_techniques_classification_and_properties)
- [22] D. Pitsa and M. G. Danikas, “Interfaces features in polymer nanocomposites: A review of proposed models,” *Nano*, vol. 6, no. 6, pp. 497–508, Dec. 2011, doi: 10.1142/S1793292011002949.
- [23] T. Tanaka, G. C. Montanari, and R. Mülhaupt, “Polymer nanocomposites as dielectrics and electrical insulation- perspectives for processing technologies, material characterization and future applications,” *IEEE Transactions on Dielectrics and Electrical Insulation*, vol. 11, no. 5, pp. 763–784, Oct. 2004, doi: 10.1109/TDEI.2004.1349782.
- [24] T. Britannica, “Polymer.” Accessed: Jan. 22, 2024. [Online]. Available:

- [25] V. Arumugaprabu *et al.*, *Polymer-Based Composites*, (1st ed). 2021.
- [26] P. Sivasubramanian, K. Mayandi, V. Arumugaprabu, N. Rajini, and S. Rajesh, “History of Composites and Polymers,” in *Polymer-Based Composites*, Boca Raton: CRC Press, 2021, pp. 1–21. doi: 10.1201/9781003126300-1.
- [27] A. Vashchuk, A. M. Fainleib, O. Starostenko, and D. Grande, “Application of ionic liquids in thermosetting polymers: Epoxy and cyanate ester resins,” *Express Polym Lett*, vol. 12, no. 10, pp. 898–917, Oct. 2018, doi: 10.3144/EXPRESSPOLYMLETT.2018.77.
- [28] “What is TPE? - Learn about Thermoplastic Elastomer Material - Kuraray.” Accessed: Jun. 22, 2024. [Online]. Available: <https://www.elastomer.kuraray.com/blog/what-is-tpe/>
- [29] A. Hiremath, A. A. Murthy, S. Thipperudrappa, and B. K N, “Nanoparticles Filled Polymer Nanocomposites: A Technological Review,” *Cogent Eng*, vol. 8, no. 1, Jan. 2021, doi: 10.1080/23311916.2021.1991229.
- [30] M. Chaharmahali, Y. Hamzeh, G. Ebrahimi, A. Ashori, and I. Ghasemi, “Effects of nano-graphene on the physico-mechanical properties of bagasse/polypropylene composites,” *Polymer Bulletin*, vol. 71, no. 2, pp. 337–349, 2014, doi: 10.1007/s00289-013-1064-3.
- [31] D. Schmidt, D. Shah, and E. P. Giannelis, “New advances in polymer/layered silicate nanocomposites,” *Curr Opin Solid State Mater Sci*, vol. 6, no. 3, pp. 205–212, Jun. 2002, doi: 10.1016/S1359-0286(02)00049-9.
- [32] F. Hussain, M. Hojjati, M. Okamoto, and R. E. Gorga, “Review article: Polymer-matrix Nanocomposites, Processing, Manufacturing, and Application: An Overview,” *J Compos Mater*, vol. 40, no. 17, pp. 1511–1575, Sep. 2006, doi: 10.1177/0021998306067321.

- [33] H. Huang, "Electrochemical Application and AFM Characterization of Nanocomposites : Focus on Interphase Properties," 2017.
- [34] K. Randazzo *et al.*, "Direct Visualization and Characterization of Interfacially Adsorbed Polymer atop Nanoparticles and within Nanocomposites," *Macromolecules*, vol. 54, no. 21, pp. 10224–10234, Nov. 2021, doi: 10.1021/ACS.MACROMOL.1C01557/ASSET/IMAGES/LARGE/MA1C01557\_0008.JPEG.
- [35] E. Senses, S. Narayanan, Y. Mao, and A. Faraone, "Nanoscale Particle Motion in Attractive Polymer Nanocomposites," *Phys Rev Lett*, vol. 119, no. 23, p. 237801, Dec. 2017, doi: 10.1103/PhysRevLett.119.237801.
- [36] H. Emamy, S. K. Kumar, and F. W. Starr, "Diminishing Interfacial Effects with Decreasing Nanoparticle Size in Polymer-Nanoparticle Composites," *Phys Rev Lett*, vol. 121, no. 20, p. 207801, Nov. 2018, doi: 10.1103/PHYSREVLETT.121.207801/FIGURES/4/MEDIUM.
- [37] K. Y. Lau *et al.*, "Modeling of polymer nanocomposites: Permittivity vs. electric field intensity," in *2014 IEEE International Conference on Power and Energy (PECon)*, IEEE, Dec. 2014, pp. 140–145. doi: 10.1109/PECON.2014.7062429.
- [38] Z. Cai, X. Wang, B. Luo, W. Hong, L. Wu, and L. Li, "Dielectric response and breakdown behavior of polymer-ceramic nanocomposites: The effect of nanoparticle distribution," *Compos Sci Technol*, vol. 145, pp. 105–113, Jun. 2017, doi: 10.1016/J.COMPSCITECH.2017.03.039.
- [39] K. Y. Lau, M. A. M. Piah, and K. Y. Ching, "Correlating the breakdown strength with electric field analysis for polyethylene/silica nanocomposites," *J Electrostat*, vol. 86, pp. 1–11, Apr. 2017, doi: 10.1016/J.ELSTAT.2016.12.021.